UPPSALA
UNIVERSITET

Digital Comprehensive Summaries of Uppsala Dissertations from the Faculty of Pharmacy 196

Microgel Interactions with Peptides and Proteins

Consequence of Peptide and Microgel Properties

RONJA WIDENBRING

ACTA
UNIVERSITATIS
UPSALIENSIS
UPPSALA
2015

ISSN 1651-6192
ISBN 978-91-554-9157-4
urn:nbn:se:uu:diva-242893

Dissertation presented at Uppsala University to be publicly examined in B21, BMC, Husargatan 3, Uppsala, Friday, 20 March 2015 at 09:15 for the degree of Doctor of Philosophy. The examination will be conducted in English. Faculty examiner: Professor Catherine Picart (CNRS, Grenoble INP).

Abstract

Widenbring, R. 2015. Microgel Interactions with Peptides and Proteins. Consequence of Peptide and Microgel Properties. *Digital Comprehensive Summaries of Uppsala Dissertations from the Faculty of Pharmacy* 196. 65 pp. Uppsala: Acta Universitatis Upsaliensis. ISBN 978-91-554-9157-4.

Microgels are lightly cross-linked hydrogel particles in the sub-micrometer to micrometer size range with a capacity to drastically change their volume in response to changes in the external environment. Microgels have an ability to bind and store substances such as biomacromolecular drugs, notably proteins and peptides, and release them upon stimuli, making them potential candidates as drug delivery vehicles and functional biomaterials. This thesis aims at clarifying important factors affecting peptide-microgel interactions. These interactions were studied by micromanipulator-assisted light and fluorescence microscopy focusing on microgel deswelling in response to peptide binding, as well as re-swelling in response to peptide release or enzymatic degradation. To evaluate peptide uptake in microgels, solution depletion measurements were used whereas the peptide secondary structure was investigated by circular dichroism. In addition, the peptide and enzyme distribution within microgels was analyzed with confocal microscopy.

Results presented in this thesis demonstrate that peptide incorporation into microgels, as well as peptide-induced microgel deswelling, increases with peptide length and charge density. In addition, results demonstrate that the peptide charge (length) rather than peptide charge density determines microgels deswelling. End-to-end cyclization is shown to not noticeably influence peptide-microgel interactions, suggesting that peptide cyclization can be used in combination with oppositely charged microgel carriers to improve the proteolytic and chemical stability of the peptide compared to the corresponding linear variant. Peptide secondary structure is found to drastically affect peptide incorporation into, and release from, oppositely charged microgels. Furthermore, it is shown that microgel charge density, peptide molecular weight, and enzyme concentration all greatly influence microgel bound peptide degradation. Of importance for applications, protective effects of microgels against proteolytic peptide degradation are observed only at sufficiently high microgel charge densities. Enzyme-mediated microgel degradation is shown to increase with increasing enzyme concentration, while an increased peptide loading in microgels causes a concentration-dependent decrease in microgel degradation.

Taken together, results obtained in this work have provided some insight into factors of importance for rational use of microgels as delivery systems for protein or peptide drugs, but also in a host of other biomedical applications using weakly cross-linked polymer systems.

Keywords: Binding, Degradation, Enzyme, Gel, Hydrogel, Microgel, Peptide, Protein, Release

Ronja Widenbring, Department of Pharmacy, Box 580, Uppsala University, SE-75123 Uppsala, Sweden.

ISSN 1651-6192
ISBN 978-91-554-9157-4
urn:nbn:se:uu:diva-242893 (http://urn.kb.se/resolve?urn=urn:nbn:se:uu:diva-242893)

Till min familj

If it looks like 'Jell-O', it must be a gel!

Dr. Dorothy Jordon Lloyd

List of Papers

This thesis is based on the following Papers, which are referred to in the text by their Roman numerals.

I **Månsson R.**, Bysell H., Hansson P., Schmidtchen A., Malmsten M. *Effects of peptide secondary structure on the interaction with oppositely charged microgels*. Biomacromolecules, (2011), *12*, 419-424.

II Bysell H., **Månsson R.**, Malmsten M. *Effects of peptide cyclization on the interaction with oppositely charged microgels*. Colloids and Surfaces A: Physicochemical and Engineering Aspects, (2011), *391*, 62-68.

III Hansson P., Bysell H., **Månsson R.**, Malmsten M. *Peptide-microgel interactions in the strong coupling regime*. The Journal of Physical Chemistry B, (2012), *116*, 10964-10975.

IV **Månsson R.**, Frenning G., Malmsten M. *Factors affecting enzymatic degradation of microgel-bound peptides*. Biomacromolecules, (2013), *14*, 2317-2325.

V **Widenbring R.**, Frenning G., Malmsten M. *Chain and pore-blocking effects on matrix degradation in protein-loaded microgels*. Biomacromolecules, (2014), *15*, 3671-3678.

I was highly involved in the planning, study design, experimental work, data analysis and writing of Paper I, IV and V. I was partly involved in the planning, study design, experimental work, data analysis and writing of Paper II and III. I did not contribute to any larger extent in the theoretical modeling performed in Paper III, IV and V.

Contents

Abbreviations

AAc	acrylic acid
AAm	acrylamide
AMP	antimicrobial peptide
APTAC	acrylamidopropyltrimethylammoniumchloride
BCA	bisinchoninic acid assay
CD	circular dichroism
CLSM	confocal laser scanning microscopy
ConA	Concanavalin A
HRP	horseradish peroxidase
pAAc	poly(acrylic acid)
p(AAc/AAm)	poly(acrylic acid-*co*-acrylamide)
pAAm	poly(acrylamide)
pLys	poly-L-lysine
PNIPAM	poly(*N*-isopropylacrylamide)

Introduction

As a result of increasing resistance development against conventional antibiotics, recent advances in molecular and cell biology have led to the development of a wide range of new biologically active macromolecules, such as protein and peptide drugs, for the treatment of human diseases. However, an effective delivery of these biomacromolecular drugs is challenging, owing to their sensitiveness to deactivation through aggregation and conformational changes, as well as to chemical and enzymatic degradation. In order to achieve a desirable therapeutic effect for these drugs, and to reach a wider therapeutic applicability, appropriate drug delivery vehicles are necessary. The delivery systems must be capable to encapsulate and protect such drugs, and furthermore, the delivery vehicles need to allow controlled and/or triggerable drug release. One approach to encapsulate and protect biologically active protein and peptide drugs is by using microgels,[1-7] lightly cross-linked hydrogel particles with an average diameter ranging between 10 nm and 100 μm. Microgels offer a range of benefits as carriers for incorporated protein or peptide drugs, such as controlled drug release, preservation of secondary and tertiary structure, avoidance of aggregation, and protection from enzymatic and chemical degradation, resulting in maintained biological activity, reduced toxicity, decreased immunogenicity, and reduction of other biological side-effects to the body.[1, 8, 9] Additionally, biodegradable microgels show advantages related to straightforward elimination of empty devices, however also a more complex system considering drug release due to degrading microgels.[10-13] If conjugated with recognition moieties, e.g., ligands for a selected receptor, microgels can furthermore be targeted to selected cell types or tissues.[14-16]

Microgels have been implemented to the design and evolvement of, for example, oral and transdermal drug delivery.[17] Due to the possibility to design microgels of very small size, they also offer opportunities in other delivery routes, for example in nasal administration or in parenteral drug delivery as injectables.[3] Finally, microgels could function as surface coatings or adhesives, with or without added drugs, if adhered to biomaterials or surgical implants to reduce chronic inflammation and to improve biocompatibility.[1, 18, 19]

Peptides, proteins and enzymes

Peptides and proteins used

Peptides and proteins are chains of amino acid residues linked by covalent peptide bonds. The length of the amino acid chain determines whether the molecule is a peptide (short chain) or a protein (long chain). The exact amino acid chain length where the border between peptide and protein lies is not precise, but a commonly used dividing line is about 50 amino acids. Not counting stereoisomers, as well as modified or non-natural compounds, there are 20 different amino acid building blocks which can be combined in numerous ways, resulting in a great variety of peptides and proteins. The structure of the amino acid sequences used in Paper I-IV are displayed in *Figure 1*, while sequences of peptides used are displayed in Table 1.

Antimicrobial peptides (AMPs) form a group of small cationic peptides (≈10-40 amino acids), which constitute a fundamental element of our immune system, displaying antimicrobial activity with bacteriostatic, microbicidal and cytolytic properties.[20, 21] Therapeutically interesting AMPs show target specificity by selectively killing bacteria and other microbes but not human cells, as a result of the dissimilar composition of bacterial and human cell membranes.[22] Furthermore, some AMPs have cytotoxic effect on tumor cells, anti-inflammatory properties, as well as immune system activation or modulation.[21, 23] Due to the favorable properties of AMPs, they have attracted considerable attention as promising therapeutics against infectious diseases. An advantage with AMPs compared to traditional antibiotics is that AMPs are less susceptible to induce bacterial resistance due to that they act on multiple targets simultaneously.[21] However, as most other peptides, AMPs are vulnerable to proteolytic degradation, conformational changes, aggregation and, deactivation. In addition, AMPs show poor distribution, frequent toxicity, and short half-life in vivo.[21] A prospective methodology to circumvent these obstacles for AMPs is to use microgels as delivery vesicles to encapsulate and protect the therapeutics. Studies on the interaction between negatively charged microgels and cationic peptides is not only beneficial in the delivery aspect, it is also highly valuable for the understanding of peptides interaction with the negatively charged surface of bacteria, specifically the interaction with the anionic lipopolysaccharide (LPS) head groups on target cells.

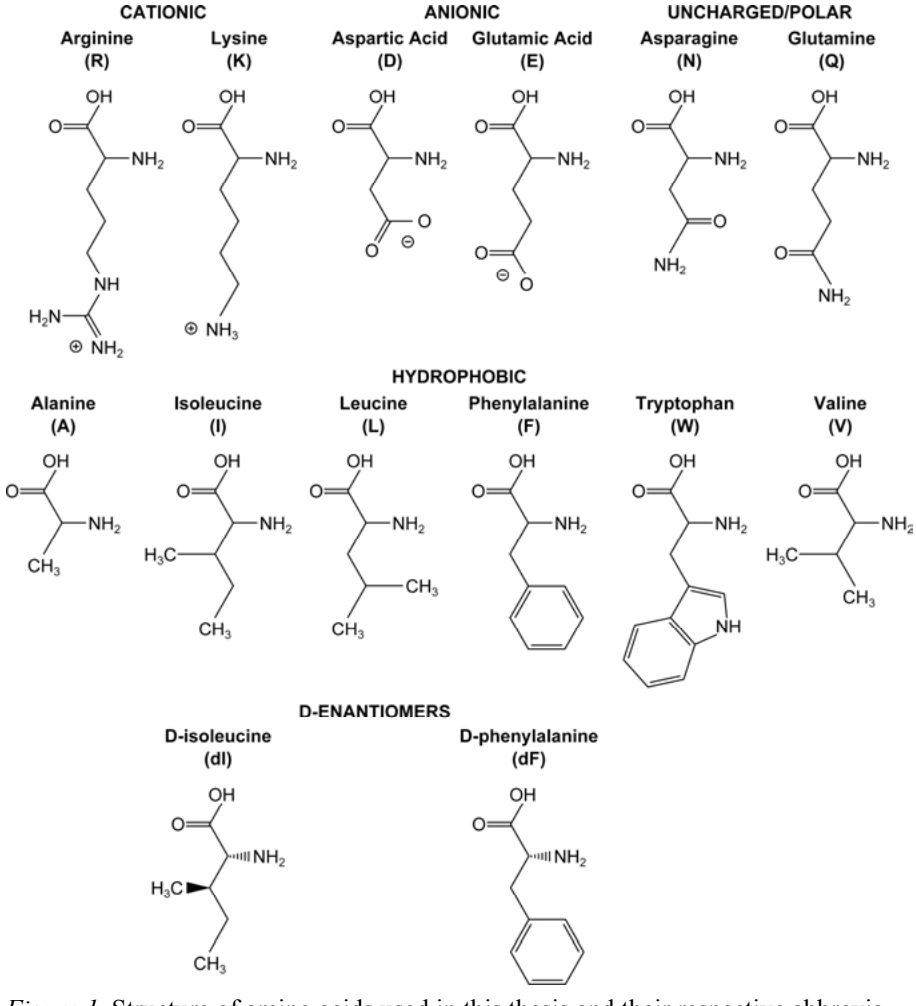

Figure 1. Structure of amino acids used in this thesis and their respective abbreviations. For isoleucine and phenylalanine, the corresponding D-enantiomers structures are shown, relevant for Paper I.

Table 1. *Properties of the studied peptides.*

Peptide	Sequence	M_w (Da)	Paper
EFK-a	CH_3CONH-E**F**KR**I**VQR**I**KD**F**LRNLV-$CONH_2$	2216	I
EFK-d/a	CH_3CONH-E**dF**KR**dI**VQR**dI**KD**dF**LRNLV-$CONH_2$	2216	I
EFK-W/a	CH_3CONH-E**W**KR**W**VQR**W**KD**W**LRNLV-$CONH_2$	2440	I
lARK8	CARKKAAKAC ARKKAAKA	1049	II
cARK8	C_____C	1047	II
lARK12	CARKKAAKAARKKC ARKKAAKAARKK	1533	II
cARK12	C_____C	1531	II
lARK16	CARKKAAKAARKKAAKAC ARKKAAKAARKKAAKA	1874	II
cARK16	C_____C	1872	II
lARK24	CARKKAAKAARKKAAKAARKKAAKAC ARKKAAKAARKKAAKAARKKAAKA	2699	II
cARK24	C_____ C	2697	II
K3	Ac-KKK-NH_2	403	III
K5	Ac-KKKKK-NH_2	659	III
K10	Ac-KKKKKKKKKK-NH_2	1300	III
K5A5	Ac-KAKAKAKAKA-NH_2	1014	III
K3A7	Ac-KAAAKAAAAK-NH_2	900	III
pLys	Amino acid: K	10 000, 30 000, 200 000	IV

In Paper I, the peptide EFK17 (EFKRIVQRIKDFLRNLV), derived from the human antimicrobial peptide LL-37, was chosen for studies of effects of peptide conformational changes on the interaction between antimicrobial peptides and oppositely charged microgels. EFK17 shows good potential as a peptide antibiotic, displaying good antimicrobial effect and low toxicity.[24, 25] More importantly for Paper I, EFK17 forms an essentially perfectly amphiphilic (idealized) helix, in which all polar/charged residues are located on one side of the helix, and all non-polar/hydrophobic residues are located on the other (*Figure 2*). In Paper I, three variants of EFK17 were investigated, i.e., the native EFK17, modified by terminal amidation and acetylation (EFK17-a), a peptide variant where the four I/F residues are replaced with the corresponding D-enantiomers (EFK17-d/a), and finally a peptide variant where the four I/F residues are replaced with tryptophan (EFK17-W/a).

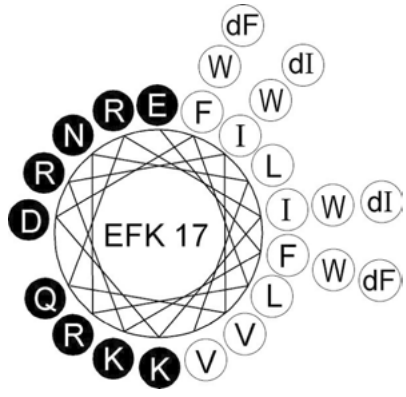

Figure 2. Helical wheel projection of EFK17 with enantiomeric (dF or dI) and tryptophan (W) substitutions outlined. Black and white circles represent charged/hydrophilic and uncharged/hydrophobic residues, respectively. Reprinted with permission from reference (24). Copyright © 2009, American Society for Microbiology.

In order to optimize peptide activity, reduce peptide proteolytic degradation, to increase peptide stability against chemical degradation, and to reach other therapeutic advantages, peptide cyclization can be used.[26] Therefore, in Paper II, the role of peptide length and cyclization on interactions with microgels was addressed by studying a series of linear and cyclic AMPs with the same repeat structure $(C(ARKKAAKA)_nC)$ (n = 1, 1.5, 2, 3), a so-called Cardin and Weintraub sequence.[27] By using this set of peptides, the peptide length can be varied without changing the sequence or peptide physicochemical properties, such as charge density and mean hydrophobicity, as well as their respective distributions within the peptides.

In Paper III and IV, the effect of peptide length was studied by lysine (K) homopolypeptides, which are peptides consisting of only one amino acid residue (K in these studies) repeated a number of times. In addition, in Paper III, copeptides of lysine with alanine (A), of varying charge density were studied.

The carbohydrate binding protein Concanavalin A (ConA) was used as a model protein drug in Paper V in order to clarify basic effects of chain and pore blocking on matrix degradation of protein-loaded microgels.

Enzymes

Enzymes are a group of biological active proteins that catalyzes selective biochemical reactions by digesting the enzymes specific substrate into smaller molecules. The enzymes used in Paper IV-V and their substrates are listed in Table 2.

Table 2. *Properties of the studied enzymes.*

Enzymes	Substrate	M_w (Da)	Paper
Trypsin	Lysine and arginine amino acid residues	23 800	IV
HRP	Several substrates, important for Paper IV is Ampliflu red	~44 000	IV
Dextranase	Dextran	41 000	V

Hydrogels and microgels

Hydrogels are cross-linked polymer networks swollen with solvent (in our case water), forming a three dimensional structure. The crosslinks are formed either by chemical or physical interactions, depending on the polymer at hand. Chemical crosslinks consists of covalent bonds and are therefore permanent (depending on chemical stability), whereas physical crosslinks, such as hydrogen bonds, or hydrophobic or ionic interactions, result in hydrogels with generally temporary crosslinks (*Figure 3*). Physically crosslinked hydrogels are therefore usually more sensitive to disintegration upon external stimuli.[5, 28, 29]

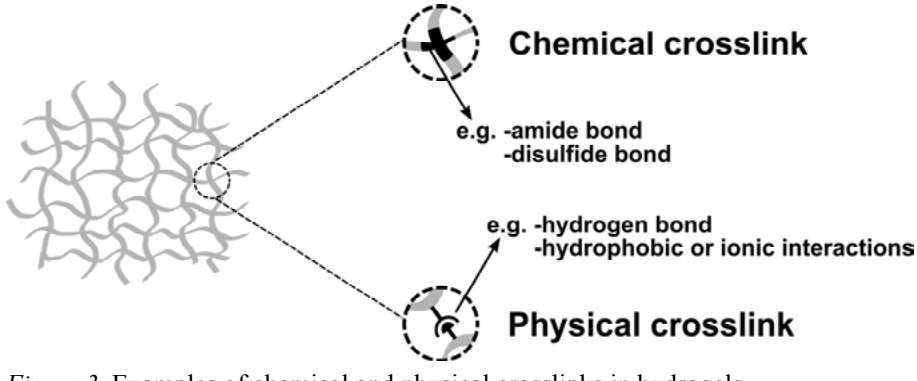

Figure 3. Examples of chemical and physical crosslinks in hydrogels.

Hydrogel networks may be characterized by a high degree of hydration, and are able to reversibly change their degree of hydration, and subsequently their volume, in response to changes in the external environment, such as pH, ionic strength, and temperature. Consequently, the hydrogel structure and viscoelastic properties can be tuned by changing either of these parameters.[29]

Hydrogels offer opportunities as biomaterials or biomaterial coatings in that they contain mostly water and have similar mechanical properties as natural (soft) tissue. If used as a biomaterial, hydrogels may therefore enhance biological interactions and improve tissue-polymer integration, all translating in potential for a good biocompatibility.[28, 30-32] Above mentioned

hydrogel properties offer a good prospective for their use in tissue engineering, biomedical implants and drug delivery. Taking drug delivery as an example, hydrogels are able to incorporate large amounts of drugs due to their highly porous structure. Additionally, due to the high water content in hydrogels, they contain an aqueous environment advantageous for maintaining the native structure and bioactivity of macromolecular drugs.[30]

The dimensions of hydrogels ranges from macroscopic to nanometer magnitudes, of these, microgels are hydrogel particles in the size-range 10 nm to 100 μm. Microgels can be prepared from a wide variety of synthetic and natural polymers. To achieve a specific microgel property, for instance a particular charge, porosity, amphiphilicity, size or degradability, the monomers, monomer ratios, and synthetic conditions can be adjusted.[33] One of the most studied microgels are those based on poly(*N*-isopropylacrylamide) (PNIPAM).[34] These microgels are thermo-sensitive and deswell with increasing temperature, resulting in either a temperature-induced "squashing release" or in drug entrapment and decreased drug release, depending on the system.[3]

Another microgel system that has been widely studied in the context of protein and peptide drug delivery is that based on acrylic acid (AAc).[1] Such microgels are prospects for pH-dependent release in oral delivery owing to their uncharged state at low pH, such as in the stomach, causing a tight network, in turn resulting in a low drug release rate. When transferred into environments with higher pH, such as in the small intestine, the acid groups dissociate and thereby cause intersegment electrostatic repulsion, in turn causing network swelling and resulting drug release. In this manner the drugs are protected from acid-catalyzed drug hydrolysis in the stomach and instead released in the small intestine where they are more stable against hydrolytic degradation.[3, 8, 35]

A slightly different group of microgels that also have been studied are biodegradable microgels, especially those derived from natural sources with high water solubility, such as chitosan, hyaluronic acid, and dextran. These carbohydrate-based biopolymers are natively biocompatible, bioactive, nontoxic and biodegradable.[5] An advantage of these biodegradable systems is that they generally are less prone to result in accumulation-related toxicity, and that surgical procedures are not required for removing them from the body after their mission, since they in the long run are cleared by degradation and resulting monomers readily excreted.

Microgel swelling/deswelling

The degree of swelling for a particular microgel depends on the specific interactions between polymer-polymer chains within the microgel and between polymer chains and the solvent. The interactions between the polymer chains inside the microgel are in turn influenced by surrounding conditions

such as, for example, temperature, pH, and ionic strength. For charged microgels, the equilibrium between the osmotic pressure and the polymer elasticity determines the degree of swelling.[36] The osmotic pressure, in turn, depends on the net difference in number of mobile ions inside a microgel and in its immediate environment.[14, 37] Distorting the osmotic pressure either inside a microgel or in its immediate environment disturbs the osmotic equilibrium, resulting in microgel swelling/deswelling until the osmotic pressure difference is equal to zero.[38] Furthermore, the swelling/deswelling will proceed until the osmotic pressure is equivalent to the sum of the elastic forces between the polymer crosslinks.[39]

Stimuli-responsive microgels

Stimuli-responsive hydrogels and microgels are able to change their chemical and/or physical properties in response to changes in their local environment such as temperature[40], electrostatics[41], specific metabolites[42, 43], external fields[44], and degradation[45], thereby allowing stimuli-responsive gels to be used for a wide range of pharmaceutical applications.[3, 46] A schematic illustration of microgel swelling and deswelling, in response to a stimulus, is displayed in *Figure 4*.

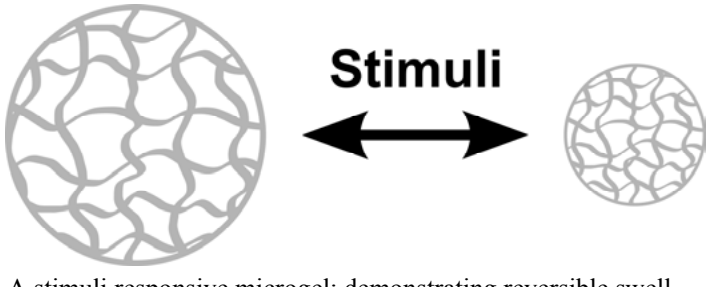

Figure 4. A stimuli responsive microgel; demonstrating reversible swelling/deswelling in response to changes in the local environment.

Triggering by electrostatics

Considerable interest has been placed on microgels displaying electrostatic triggering, for example by pH or ionic strength. In general, pH responsive microgels consist of polymer chains carrying weakly charged groups which can either accept or donate protons in response to changes in the external pH. This proton charge shift affects the hydrodynamic volume of the polymer chains through changes in the osmotic pressure, induced by mobile counter ions neutralizing the polymer charges, as well as charge-charge (Coulombic) repulsion.[46] Additionally, pH-responsive microgels can be triggered by changes in ionic strength; increased ionic strength induces increased screening of repulsive electrostatic interactions, resulting in deswelling.[46] Microgels containing acrylic acid (AAc) are one example of a pH- and

ionic strength-responsive system that has been broadly studied. At low pH, most AAc groups are uncharged (pK_a for the isolated acrylic acid group being ≈4.7), whereas at high pH the AAc is ionized resulting in network swelling, as demonstrated in *Figure 5*. To balance the internal electrostatic repulsion between AAc groups at high pH, the mobile counter-ion concentration inside the microgel is increased, resulting in an osmotic pressure shift until the overall microgel charge, including their counter-ions, is equal to zero.[39] An increase in ionic strength, on the other hand, results in deswelling for these systems due to a decreased osmotic pressure difference between the microgel interior and exterior.[37, 39]

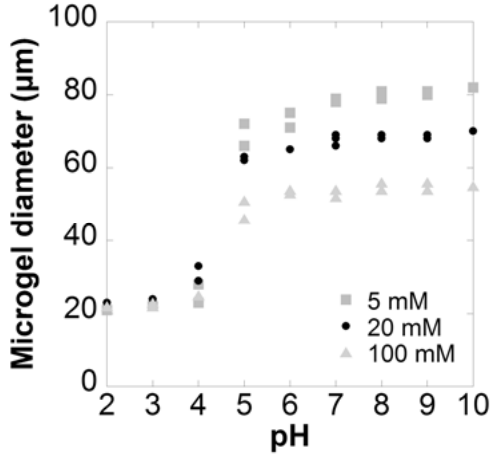

Figure 5. Swelling behavior of pAAc microgels as a result of pH variations, at different salt concentrations, based on experimental results from Paper III.

Triggering by metabolites

Apart from electrostatic triggering, there is interest in microgels displaying triggering in response to the concentration of a specific metabolite. One of the most widely studied systems in this area is that responsive to glucose concentration. For example, insulin can be incorporated in microgels based on the sugar binding protein Concanavalin A (ConA) and dextran, where ConA act as a cross-linker between dextran chains. These microgels show an insulin triggered release when exposed to glucose due to the competition between dextran and free glucose for ConA, resulting in rupture of gel cross-links when glucose binds to ConA, in turn causing insulin release.[3, 47]

Triggering by degradation

Another type of stimuli-responsiveness is that triggered by degradation. These microgels are based on polymers and/or crosslinks which can be degraded either chemically, e.g. by hydrolysis, or enzymatically. Enzymatically degradable microgels are of special interest due to the fact that they can be

used for targeted drug delivery more broadly than those depending on localized pH, ionic strength, or temperature. The concentration of a specific enzyme is dependent upon cell and tissue type and can, for example, be overexpressed in certain tumor cells, allowing for local triggered drug release.[32] For example, polysaccharide gels could be used for the treatment of colon cancer or Crohn's disease, owing to that the gels could be designed to be degraded by colon-specific enzymes, thereby inducing localized drug release.[8] Another example of this type of biodegradable system, is that based on hyaluronic acid that can be degraded by the enzyme hyaluronidase, known to be overexpressed in various cancer cells, for example in breast cancer.[48] By the above designs, the drugs are protected inside the gels until they reach their target and a localized drug release can be induced.

Microgels as biomaterials

Microgels in protein and peptide drug delivery

As mentioned, microgels can be used as delivery system for biomacromolecular drugs, such as proteins and peptides, however, also for DNA and siRNA. Some of the most critical parameters for drug loading and release from microgels are microgel size, cross-linking density, network homogeneity and degree of swelling.[3] For example, the higher the microgel crosslinking density, i.e., the more crosslinks per volume, the smaller the mesh size, resulting in a decreased swelling ratio and a slower drug release rate.[3] Particularly for larger drugs, such as proteins and DNA, mesh size restrictions may also impair drug incorporation throughout the microgels, resulting in reduced drug load.

Peptide or protein loading and release from microgels can be achieved by self-assembly mechanisms involving non-covalent interactions, e.g., through electrostatic interactions, hydrogen bond formation or hydrophobic interactions. Taking polylysine and pAAc microgels as an example and looking at the pH dependence of the lysine groups, drug loading through electrostatic interactions by alternating pH can be demonstrated. At pH values lower than the peptides isoelectric point (pH 9.7 for isolated K), lysine is positively charged, whereas at pH values above the isoelectric point, lysine is uncharged. When fully charged at low pH values, the peptide will bind readily to the oppositely charged microgel, inducing extensive microgel deswelling. At sufficiently high pH values the peptide is uncharged, while the microgel becomes uncharged at sufficiently low pH, in both cases reducing electrostatic peptide-microgel interactions, facilitating peptide release.

An alternative to drug loading by non-covalent interactions is to immobilize the drug in the microgel through covalent bonds between the drug and polymer during microgel synthesis. An advantage of using drug self-

assembly loading over covalent drug binding is that the microgels can be synthesized and evaluated in the absence of the drugs.[14]

Microgels on surfaces

Microgels, with or without encapsulated drugs, can be used for functionalization of surfaces, for example, to promote tissue-cell interactions and hinder the adhesion of bacteria to biomedical devices. So far, there has been relatively little work done on microgel adsorption/immobilization to biomaterial surfaces, despite considerable potential in the area. For example, poly(ethylene glycol)-*co*-acrylic acid based microgel adsorption to surfaces, both with and without antimicrobial peptide loading, has been shown to hinder bacterial colonization, offering possibilities for reduced biomaterial associated infection.[49] In addition, microgels based on the same monomers have, when adsorbed to surfaces, shown enhanced osteoblast spreading, metabolic activity, and motility, translating in probability in faster healing after implantation.[50] Taking together, these examples demonstrate that microgels could be used to improve the biocompatibility of a surface of, for example, an implant or any other biomedical device.

Biocompatibility

The term biocompatibility can be defined as the ability of a material to perform its desired function without provoking undesirable local or systemic side effects.[51] Microgels with high water content and structural similarities with soft human tissue (such as connective tissues, ligaments, blood vessels etc.), as well as their resulting low interfacial tension and high hydrophilicity, is beneficial for biomaterial applications considering that a biocompatible microgel must have the ability to coexist with human tissues without causing an unacceptable degree of harm.[6, 51] However, there are several criteria that a microgel must meet in order to be biocompatible, such as absence of undesired cytotoxic effects and good tissue and blood compatibility.[6, 52]

Studying the interactions between microgels and peptides/proteins is important for the understanding of microgels biocompatibility capacity, considering that plasma protein adsorption to a biomaterial is the first process that occurs when a foreign surface is placed in contact with blood.[52] The protein adsorption in turn affects the amount and type of a followed platelet adhesion and activation, which in turn affects an initiated coagulation and complement cascade, including macrophage attraction, demonstrating that protein adsorption to a biomaterial surface is important for the recognition by cells and tissues.[52-54] The material type, hydrophobicity, charge, and surface properties, among other, of a biomaterial affect the protein adsorption, and consequently the adhesion and activation of macrophages and other cell types. For instance, hydrophilic surfaces are shown to suppress protein ad-

sorption more than their hydrophobic counterparts, resulting in decreased platelet adhesion and macrophage attachment.[53, 55] Furthermore, hydrophilic and anionic materials have demonstrated to induce increased apoptosis (programmed cell death) of adhered macrophages compared to hydrophobic or cationic materials.[56]

Small microgels, and other nanomaterials, placed in biological environment, such as into blood, will endure a bit different fate compared to larger biomaterials, due to their high surface to volume ratio, their distribution throughout the body where they will come upon several cell types, and their small size which could induce cell endocytosis.[57, 58] The surface of a nanoparticle will be covered by plasma proteins once incorporated into physiological environments and a "protein corona" formed, modifying the particles size and interfacial properties.[57, 58] The outcome of the nanoparticle is decided by the corona composition rather than the nanoparticle composition, consequently, identification of the absorbed proteins conformation and lifetime is important.[57] For nanoparticles, a cationic net charge of the particle has shown to induce fast clearance from blood due to opsonization (opsonin/protein absorption) resulting in removal of the particle by macrophages in the reticuloendothelial system.[57]

Microgel degradation

Degradation of biodegradable microgels can be achieved either by surface or bulk erosion (*Figure 6*), or by a combination of these two mechanisms, depending on the system at hand. The mechanism of erosion depends on factors such as rate of water diffusion inside the network, rate of polymer chains scission, and the matrix dimensions. Surface erosion is the primary degradation mechanism when water and enzyme diffusion within the gel is slower than polymer chain scission. This is a desirable mechanism for most drug delivery systems since it allows for reduction of burst release, as well as for a continuous drug release.[59]

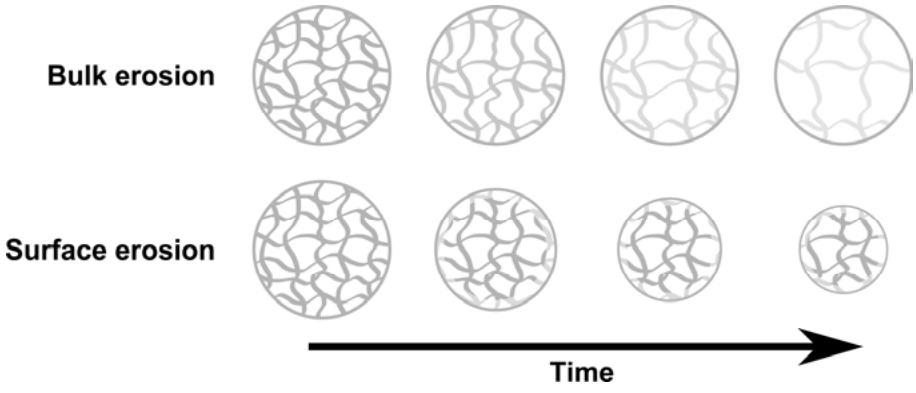

Figure 6. Representation of two separate microgel matrixes enduring two different degradation mechanisms.

Parameters affecting degradation kinetics, such as degradation rate and mechanism, are for example, nature of the crosslinks and scissions, microgel cross-linking density, pore size, and diameter, and environmental conditions such as pH, ionic strength, temperature, and enzyme concentration. For a biodegradable microgel, it is important that the degradation kinetics are well controlled and that the degradation products are biocompatible without provoking any side effects, such as inflammation or a cytotoxic response.[32]

Aim of the thesis

The overall aim of this thesis was to clarify important factors affecting peptide incorporation into, distribution within, and release from, sparsely cross-linked polyelectrolyte microgels, and how these factors depend on peptide and microgel properties. In addition, the thesis aimed to provide some insight into parameters affecting proteolytic degradation of microgel-loaded peptides, and of the microgel matrix in the presence of a peptide/protein load. For these systems, specific focus was intended to be placed on how parameters such as:

- peptide secondary structure, conformation, cyclization, and molecular weight
- peptide, enzyme and metabolite concentration
- microgel charge density
- pH
- ionic strength

impact the interaction between peptides/proteins and polyelectrolyte microgels.

Methods

Microgel synthesis

Inverse suspension polymerization

Acrylic acid/acrylamide (AAc/AAm) microgels were synthesized by inverse suspension polymerization, using a coarse water-in-oil emulsion. In a water-in-oil emulsion, polymerization takes place inside aqueous droplets containing monomer and cross-linker. To achieve these aqueous droplets, water and water-soluble monomers and cross-linkers were emulsified, by stirring, in a continuous oil phase containing oil-soluble surfactants. To synthesize the studied p(AAc/AAm) microgels (PaperI-IV), cyclohexane was used for the continuous phase together with the oil-soluble surfactant Span 60 (sorbitan monostearate), the latter used for colloidal stability. With these components, stable spherical droplets are formed and the charge content in the forming spherical microgels can be controlled by varying the ratio of AAc/AAm in the water soluble monomer solutions. As an accelerator, initiator and cross-linker, TEMED (*N,N,N′,N′*-tetramethyl-ethylenediamine), APS (ammonium persulfate) and BIS (*N,N′*-methylenebisacrylamide) was used, respectively.[60] In addition to p(AAc/AAm) microgels, in Paper IV, quaternary ammonium salt microgels were also studied. These microgels where synthesized with the same polymerization technique and same additives as described above, with the exception that the monomers where replaced with APTAC (acrylamidopropyltrimethylammoniumchloride).

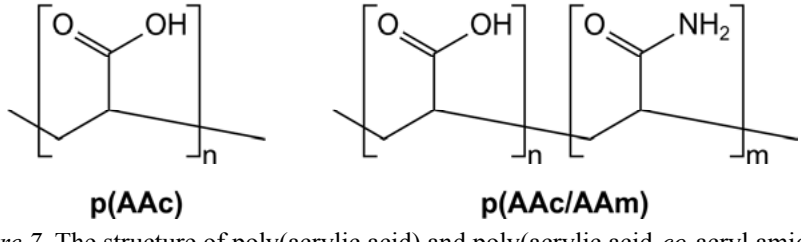

Figure 7. The structure of poly(acrylic acid) and poly(acrylic acid-*co*-acryl amide)

A drawback with this emulsification technique is that the obtained microgels show a very wide size distribution due to polydispersity of the emulsion droplets during the polymerization process.[6] Therefore, the p(AAc/AAm) microgels where fractionated by sieving to reduce the size distribution.[60] In

addition, individual microgel particles were examined in order to allow studies of microgels with a narrow size distribution. For future studies, microgels with a controlled size and a uniform size distribution would be preferable. One approach to receive better controlled droplets and microgels is to use microfluidic techniques that provide precise emulsification of polymer solutions followed by physical or chemical cross-linking resulting in microgels with controlled particle shape, size and porosity.[4, 61]

Biodegradable microgels

To study biodegradable microgels, dextran, a polydispersed high molecular weight polysaccharide, consisting predominantly of α-1,6 glucosidic linkages, was chosen due to previously shown good biocompatibility and slow biodegradability for dextran based microgels.[62-64] Microgels based on dextran may be hydrolyzed by the enzymes dextranases that cleaves the glucosidic linkages,[65, 66] generating linear oligosaccharides.[62, 67-70] Dextranases are found in several organs in the body, such as in the liver, spleen, kidney, and colon, all displaying characteristic enzyme activity.[71, 72] However it is not present in blood to any larger extent, providing some opportunities for targeted drug delivery. Consequently, dextran-dextranase systems have previously been considered for controlled and targeted release of drugs from dextran hydrogels.[64, 68, 73-77] An advantages offered by this dextran-dextranase system is that dextranase degrades only the matrix and not incorporated proteins.

The biodegradable dextran microgels/microparticles studied in Paper V were Sephadex G-200 (Particle size: 40-120 μm), obtained from Pharmacia Fine Chemicals AB (Uppsala, Sweden). Although being more highly cross-linked and less responsive than many traditional microgels, these are nevertheless highly swollen and water-rich, and therefore referred to as microgels in this work for convenience.

Peptide-microgel interactions by microscopy

Micromanipulator-assisted light microscopy

Light microscopy was used as a major tool in this work to study the kinetics of peptide-microgel interactions by imaging microgel phase transformations. Light, or optical, microscopy is a microscopy technique which involves visible light and a lens system used to magnify small samples. To the microscope used in this thesis, a digital camera is connected, which enables digital imaging of the studied microgels.

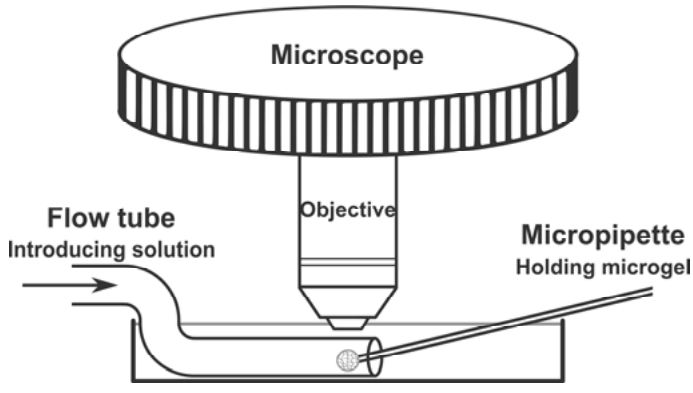

Figure 8. Schematic of the micromanipulator-assisted light microscopy experimental setup.

Peptide-microgel interactions were studied by micromanipulator-assisted light and fluorescence microscopy focusing on the microgel deswelling in response to peptide binding and re-swelling in response to peptide release or in response to enzymatic degradation. With the experimental setup used in this method, a single microgel particle is captured with a micropipette attached to a micromanipulator, and suction is used to hold the microgel steady against the pipette (*Figure 8*). Once fixed to the pipette, the microgel is transferred into a flow tube and flushed with any desirable solution at a constant and controllable flow rate. This experimental setup ensures that the solute composition surrounding the microgel remains constant and unaffected by solution uptake in gels, and enables switching of solution composition (e.g. peptide and enzyme concentration) during the run of the experiment. Furthermore, the setup provides laminar flow with a controllable (flow-dependent) unstirred layer thickness, enabling theoretical analysis of diffusion.[78] Captured microgel particles is photographed and analyzed by measuring the microgel diameter and converting it to volume, with the assumption of a perfect sphere (Paper I-IV), or by measuring the volume of a perfect sphere directly from the microscopic image (Paper V). The microgel volume ratio is expressed as V/V_0, were V is the volume of a gel particle after buffer or enzyme exposure for a certain time, and V_0 is the volume of a gel particle in a specified reference solution (*Figure 9*).

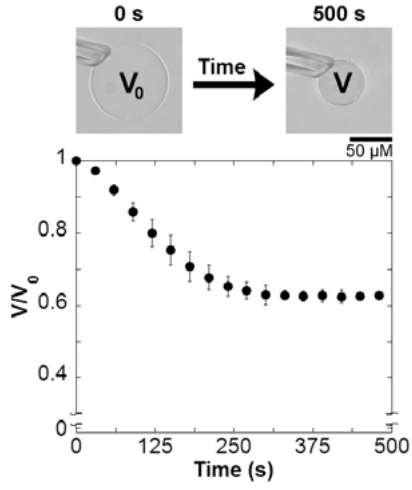

Figure 9. Kinetics of peptide induced microgel deswelling and exemplifying microscopy images for 25% p(AAc/AAm) microgels upon the addition of 5 µM pLys (10 kDa) at 150 mM ionic strength, pH 7.4. (Results from study IV not included in the paper)

Peptide binding

In Paper I, II, and IV microgel deswelling upon peptide binding was studied by micromanipulator-assisted light microscopy by flushing the microgel with peptide solution of 5 µM until the microgel volume change stagnated. It was assumed that when the microgel stopped deswelling, the microgel-peptide solution was at equilibrium and the microgel was fully loaded. In Paper III, the microgels where instead exposed to peptide solution of increasing concentration by flushing with peptide solution for 30 minutes at each concentration. Peptide induced microgel kinetic deswelling curves are in all cases obtained by plotting deswelling ratios (V/V_0) versus time (t), as demonstrated in *Figure 9*. In Paper V, peptide-induced microgel deswelling was exceptionally slow, leading to long experimental times, resulting in unacceptably high peptide amount required to be able to perform the experiments. Instead a microgel solution where therefore equilibrated with peptide solution for 24 h in this case, to reach saturation peptide uptake.

Peptide distribution

In addition, micromanipulator-assisted light microscopy experimental setup also provides for analyzes with fluorescence microscopy with the addition of a UV-lamp. In Paper I, this was utilized to analyze the peptide distribution during and after microgel deswelling by monitoring the autoflorescence of tryptophan residues in the studied peptide (thus requiring no fluorescent labeling). However, fluorescence analysis with the light microscope used is limited, since fluorophores throughout the entire microgel volume are illuminated, leading to the collection of fluorescent signals not only from the

plane of focus (as in confocal microscopy), but from the entire microgel, resulting in blurry images.

Peptide release

After completion of peptide binding in Paper I-III, microgels were flushed with a solution of high salt concentration (150 or 200 mM). When exposed to high ionic strength, peptide detachment from microgels is induced as a result of decreased electrostatic attraction between peptide and microgel matrix. As an effect of peptide detachment, the microgel will re-swell. However, due to electrolyte-dependent swelling/deswelling, it will not re-swell to its original volume as long as the microgel is exposed to high electrolyte concentration considering the high free ion concentration inside and outside the microgel. To be able to compare the original volume with the volume after peptide detachment, the microgel was therefore flushed with buffer solution of the same ionic strength as the reference state. This will cause a decrease in the free ion concentration inside the microgel and the electrostatic repulsion between the charged groups in the microgel will increase, causing network swelling. In *Figure 10* peptide binding to, and release from, microgels is illustrated.

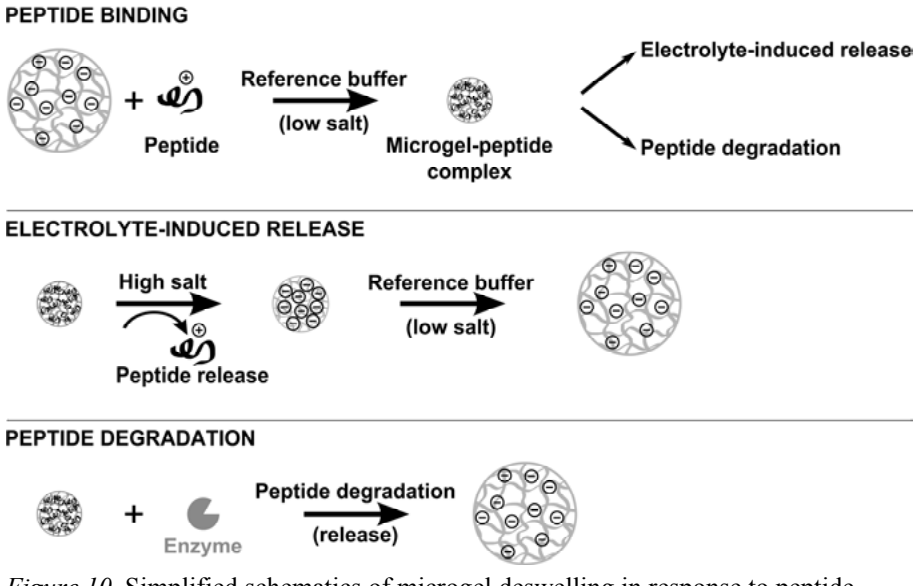

Figure 10. Simplified schematics of microgel deswelling in response to peptide binding and re-swelling in response to peptide release or degradation (counter-ions are not illustrated).

Peptide degradation

Peptide release from microgels induced by enzymatic peptide degradation was as also studied by micromanipulator-assisted light microscopy (Paper

IV). In this case, microgels were flushed with enzyme solution of various concentrations after peptide binding until the microgels were fully swollen again and all peptide (residues) were desorbed due to degradation (*Figure 10*, bottommost).

Microgel degradation

In Paper V, micromanipulator-assisted light microscopy was furthermore used to study changes in microgel volume upon enzymatic degradation of the microgel matrix. This was studied by flushing a single microgel (void or peptide-loaded) with enzyme solution of various concentrations until the microgel was completely disintegrated.

Confocal laser scanning microscopy

Confocal laser scanning microscopy (CLSM) was used to image and analyze peptide and enzyme distributions within microgels. As used in the present investigation, CLSM is a fluorescence microscopy technique, which enables imaging of thin optical sections of a fluorescent sample by focusing light from a laser onto the plane of focus (focal plane) and collecting the emitted fluorescent signal via confocal pinholes by a photodetector coupled with a photomultiplier tube (PMT). The confocal pinhole eliminates emission from above and below the plane of focus, whereas emission from the plane of focus passes through and is detected by the photodetector (*Figure 11*). The instrument used in this thesis is equipped with three lasers (488, 543, and 633 nm), and a spectral imaging detection system that enables simultaneous analysis of fluorophores with overlapping spectra through control of the bandwidth of the emission uptake. By combining this detector with sequential scanning by individual lasers and detecting the fluorescent signal in each channel, the potential of bleed through artifacts is minimized, and two (or more) fluorophores in one sample can be viewed simultaneously. In Paper IV-V, bleed-through was additionally diminished by choosing fluorophores with well separated absorption and emission spectra.

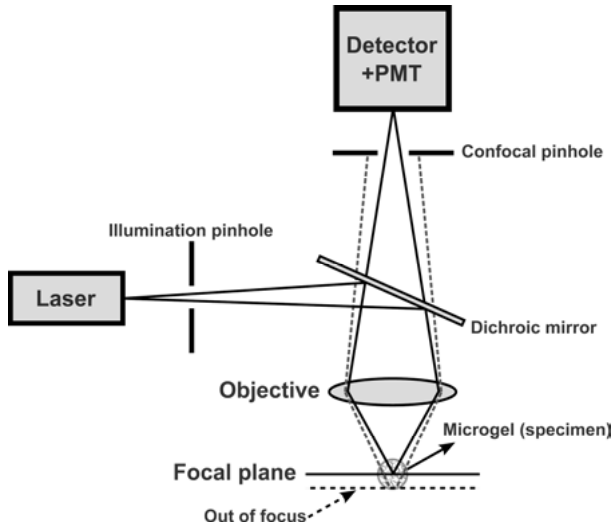

Figure 11. Schematic of the CLSM.

Fluorescent labeling

In Paper IV-V the peptides and enzymes where fluorescently labeled to be able to be visualized by CLSM. The fluorescent labels used in this thesis were Alexa Fluor® 488 and 633 (Table 3), both amine-reactive succinimidyl esters. Alexa Fluor® 488 is a green fluorescent dye, allowing excitation to be executed with a 488 nm laser, whereas Alexa Fluor® 633 is a red fluorescent dye where excitation can be executed with a 633 nm laser. Fluorophore labeling was performed by mixing the peptide or enzyme with the dye under basic conditions for one hour. Thereafter, unbound fluorescent molecules where separated from the peptide/enzyme-bound complexes by a gel filtration column. To determine the dye concentration in the final solution, spectrophotometry measurements where performed, while the final peptide or enzyme concentration was determined by BCA assay. Finally, the labeling density was obtained from these two concentrations (dye/peptide or enzyme molar ratio).

Table 3. *Properties of the fluorescent labels used in the thesis.*

Conjugate	Excitation maxima (nm)	Emission maxima (nm)	M_w (Da)
Alexa Fluor® 488	495	519	643.4
Alexa Fluor® 633	632	647	~1200

Attaching a rather large fluorescent label to a peptide or enzyme might potentially affect peptide and enzyme physicochemical properties. However, labeled and unlabeled polylysine was previously found to result in similar microgel deswelling.[79] In addition, comparable findings were found in Paper IV with structurally different Alexa 488 and 633, and a good correlation

found between results on the effects of molecular weight, enzyme concentration, and microgel charge density for confocal microscopy (using labeled compounds) and micromanipulator-assisted light microscopy (using unlabeled compounds). This indicates that the effect of labeling is not important (at these labeling densities) for the presently investigated systems.

Peptide and enzyme distribution in microgels

To determine peptide distributions in microgels, as well as microgel-bound peptide degradation kinetics, fluorescently labeled peptides were mixed with microgel solution and equilibrated for at least 24 h. Thereafter, loaded microgels were monitored by CLSM and the fluorescent distribution and intensity within the microgel particles analyzed. To quantify this distribution, intensity profiles through the middle section of the microgels were obtained, and to determine the average intensity in single microgels, region of interest (ROI) analyses were performed.

Peptide degradation

Peptide detachment induced by enzymatic degradation in single microgel particles was investigated in Paper IV by mixing peptide-microgel solution with enzyme solution, directly followed by CLSM monitoring and analysis. In doing so, the intensity ratio is expressed as I/I_0, were I is the intensity of a gel particle after enzyme exposure for a certain time, and I_0 the intensity of a gel particle at the first measurement (four minutes) after mixing with enzyme solution.

Microgel degradation

Enzyme and peptide distribution during degradation of single microgel particles was studied in Paper V by mixing peptide-microgel solution with enzyme solution. The resulting mixture was monitored directly thereafter by CLSM and intensity profiles obtained as described above.

Bisinchoninic acid assay

An assay with the stable, water-soluble compound bisinchoninic acid (BCA) was used for peptide concentration quantification. The basis of this method consists of two steps. In the first step, present peptide bonds (and the amino acids tyrosine, cysteine, and tryptophan) react with Cu^{2+} ions in alkaline conditions, resulting in Cu^{+} ions in a concentration-dependent manner (*Figure 12*). In a second step, BCA forms an intense purple complex with Cu^{+} ions which is conveniently measured at its absorbance maximum at 562 nm. The absorbance thus measured is proportional to the amount of peptide present ,allowing peptide concentration determination.[80]

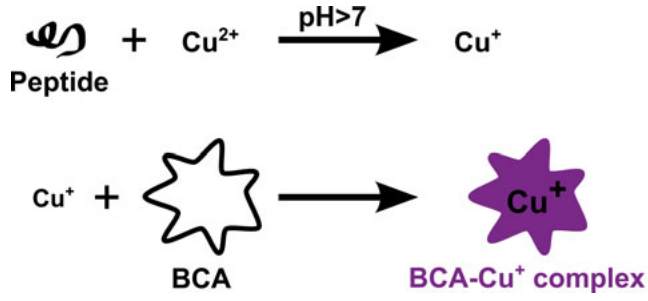

Figure 12. The two steps in the purple BCA-Cu^{+} complex formation.

Uptake measurements

Peptide uptake in microgels was quantified using a solution depletion method in Paper I-II. For this purpose, microgel solutions were equilibrated with peptide of various concentrations for at least 48 h. The microgel-peptide complexes thus formed were thereafter separated from solution by centrifugation and the concentration of peptide remaining in solution determined by BCA assay (*Figure 13*). By comparing the peptide concentration remaining in solution after equilibration with microgels to that of a control solution without added microgels, the adsorbed amount of peptide per mass microgel is straightforwardly obtained.[81]

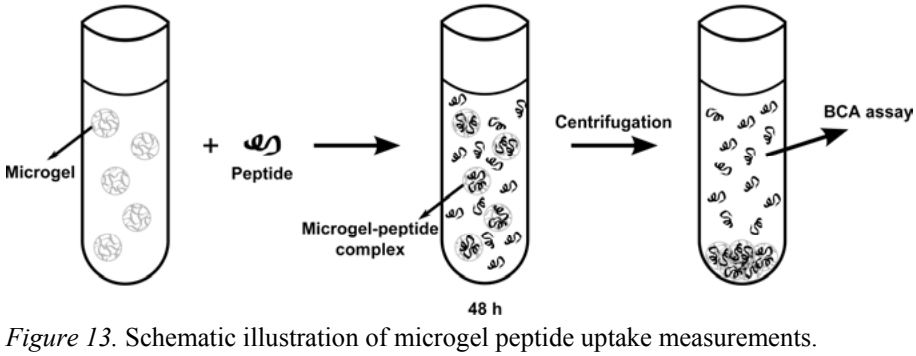

Figure 13. Schematic illustration of microgel peptide uptake measurements.

Spectrofluorometry

To demonstrate the absence of peptide aggregates in aqueous solution, and when bound to microgels, a fluorescence spectroscopy was used in Paper I. By monitoring the autoflorescence of tryptophan residues in the studied peptide and analyzing the resulting fluorescence spectra, it can be estimated whether or not the peptide is exposed to a polar environment. The emission wavelength maxima of tryptophan shifts when the polarity of the surround-

ing changes, allowing for peptide aggregation estimations. If aggregates are formed, the tryptophan residues would be surrounded by a non-polar environment inside the protein aggregate (resulting in a blue-shift of the fluorescence maximum), as opposed to the polar surroundings for tryptophan in aqueous solution.

Circular dichroism

Circular dichroism (CD) spectroscopy was used to monitor peptide conformation in solution and when incorporated into microgels (Paper I-II). With CD measurements the secondary structure, folding, and binding properties of a peptide or protein can be evaluated by quantifying the differential absorption of left-handed and right-handed circularly polarized light.[82] Different structural elements have characteristic CD spectra, furthermore, a specific peptide secondary structure will result in a distinctive CD-spectra. Therefore, if a CD signal for an unknown peptide structure is compared to a spectra for an identified secondary structure the fraction of peptide conformation can be determined. In Paper I-II, the equation below was used to evaluate the fraction of α–helical conformation,

$$X_\alpha = \frac{A - A_c}{A_\alpha - A_c}$$

where A is the recorded CD signal at 225 nm and A_c and A_α is the CD signal at 225 nm for a reference peptide in a 100% random coil and in a 100% α-helix conformation, respectively.[83, 84]

Activity assay

Peptide activity

To compare peptide activity before and after enzyme exposure in Paper IV, a combination of horseradish peroxidase (HRP) and Ampliflu red together with CLSM analysis was used. This method was used to quantify that the HRP biological activity is retained once bound to microgels and further to quantify if the enzyme degrades the microgel-bound HRP to such extent that its activity is diminished. The basis of this method is that Ampliflu red, a non-fluorescent HRP substrate, is converted to resorufin, a fluorescent compound, in the presence of active HRP and hydrogen peroxide (*Figure 14*). The amount of released resorufin can be visualized by CLSM imaging, where the degree of intensity can be set equivalent to the grade of activity, and where non-detectable intensity corresponds to no activity.

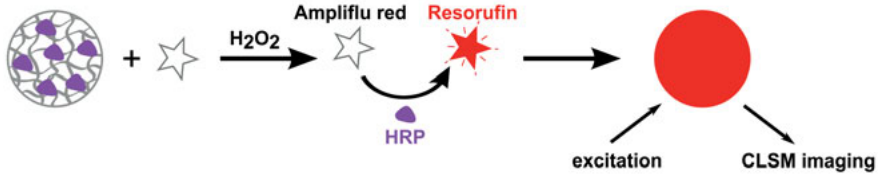

Figure 14. Demonstrating how the presence of active HRP turns the microgel fluorescent red in the CLSM.

Enzyme activity

Enzyme activity was measured by using the method of Koh and Khouw for dextranase activity on dextran in Paper V.[66] The basis of this technique is measurement of the consumption of substrate by monitoring the amount of released dye complex (Cibacron Blue[67]) from an excess of the substrate Blue Dextran 2000. The rate of conversion of dextran-bound Cibacron Blue dye (ethanol-insoluble) to an ethanol-soluble form on dextran digestion by dextranase can be measured by reading the absorbance, as demonstrated in *Figure 15*.[66, 67] The amount of released dye can subsequently be set equivalent to the degree of activity.

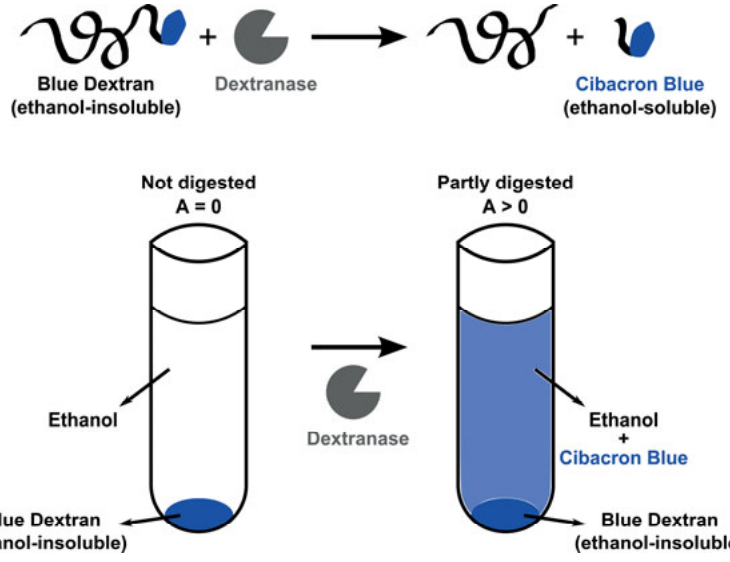

Figure 15. Schematic illustration of how dextranase digestion of Blue Dextran results in an increase in the absorbance (A).

Results and discussion

Effect of peptide variations

The major driving force for peptide binding to microgels is electrostatic attraction. This is not to say, however, that the interactions are not affected by other features. Binding of peptides to microgels is highly influenced by the peptide characteristics. Factors such as peptide length, cyclization, structure and hydrophobicity may all effect the interactions between peptide and microgel. For that reason, these aspects will be discussed below, based on the findings in Paper I-IV for positively charged peptides interacting with negatively charged microgels.

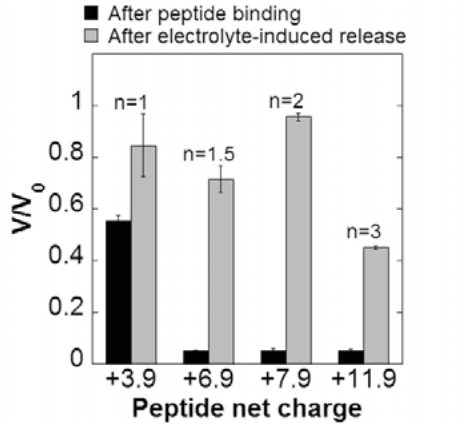

Figure 16. Final volume ratio, V/V_0, in 20 mM ionic strength, pH 7.4, of 50% p(AAc/AAm) microgels after exposure to 5 μM linear $(ARKKAAKA)_n$ with varied peptide sequence repetition (n) (black), followed by rinsing with buffer solution of 150 mM (grey). (Paper II)

Peptide length and charge density

In Paper II, variants of peptide oligomers with similar charge density and mean hydrophobicity were studied focusing merely on effects of peptide length. As shown in *Figure 16*, an increased microgel deswelling (due to an increased peptide binding) can be seen with increasing peptide length (increasing peptide sequence repetition) for the $(ARKKAAKA)_n$ peptides investigated. The longer the peptide, the higher the net charge, and the larger

the electrostatic driving force for binding to microgels. Also at constant charge density, however, there is an increased driving force for polyelectrolyte and peptide binding due to a smaller translational entropic penalty on adsorption for longer peptides.[23] Analogous to binding at low ionic strength, decreased electrolyte-induced peptide desorption by electrostatic screening is seen with increasing peptide length (*Figure 16*). The main reason for the latter is the low probability for concurrent desorption of all amino acid monomers bound to the microgel network with an increasing number of monomers. Similarly to the linear $(ARKKAAKA)_n$ peptides, this length-dependence was seen also for the corresponding cyclic peptides, as demonstrated in Paper II. Furthermore, these correlations between peptide length/charge and peptide binding and release are in line with previously studies on consensus peptides and pAAc microgels.[85]

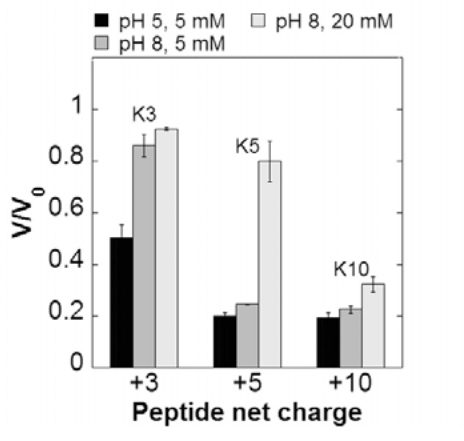

Figure 17. Final volume ratio of pAAc microgels after exposure to pLys of different length (K3, K5, and K10) and altered peptide net charge, at varied pH and ionic strength. (The final volume ratio is set equivalent to the volume at the highest peptide concentration examined in Paper III)

In Paper III, a series of lysine oligopeptides and lysine/alanine co-peptides of varying charge density were chosen for investigating effects of peptide length and charge density. As shown in *Figure 17*, the same phenomenon as shown for the $(ARKKAAKA)_n$ peptide series were seen for these peptides, where an increased number of lysine units results in an increased peptide net charge and correspondingly in an increased peptide-induced microgel deswelling.

If the peptide length is instead kept constant and peptide charge density varied by varying the lysine monomer ratio, studies of the charge density dependence of peptide-induced microgel deswelling are possible. The microgel deswelling caused by peptide binding and network neutralization increases with increasing peptide charge density, as demonstrated in *Figure*

18 a, an effect that increases with peptide concentration. Doing the opposite, and keeping the total peptide charge constant, but increasing the peptide length by incorporating uncharged alanine monomers between the charged lysine monomers, it can be clarified that the net charge of the peptide is more important than the charge density. This is demonstrated in *Figure 18 b* where the peptides K5 and K5A5, with the same net charge, show analogous peptide-induced microgel deswelling even though K5A5 have a lower charge density. Moreover, in Paper III, a theoretical model based on charge interactions between peptide and network was able to capture these experimentally observed effects semi-quantitatively, and further demonstrated that the peptide charge (length) rather than peptide charge density, determines microgel deswelling.

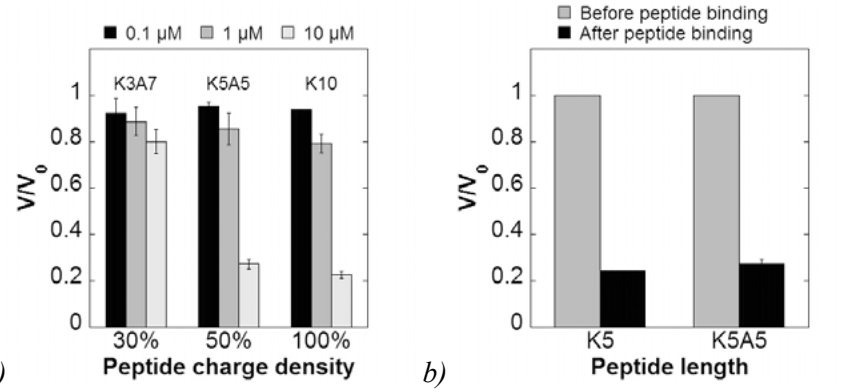

Figure 18. Final volume ratio of pAAc microgels in 5 mM ionic strength, pH 8, after exposure to increasing peptide concentrations, for different peptide charge densities (a) and peptide lengths (b). In (b), final volume ratio is shown at 10 µM (black). (Paper III)

The same length dependence correlation can be seen also for longer peptides. In *Figure 19* it is demonstrated that the total time until complete microgel collapse is decreased with increasing peptide molecular weight, for pLys peptides incorporated into p(AAc/AAm) microgels. Complicating direct comparison with results for short peptides in this case, however, is the fact that there is an M_w-dependent cut-off for network entry of the peptides, such that peptides of high molecular weight (size larger than the network mesh size) are excluded from the microgel core, and restricted to its surface.

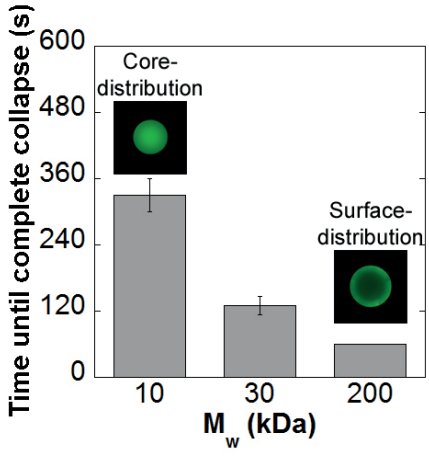

Figure 19. Time until complete microgel collapse, thereafter no further deswelling is observed, for 25% p(AAc/AAm) microgels exposed to pLys of varied molecular weight in 150 mM ionic strength, pH 7.4. The CLSM images in the insets, displays the peptide distribution in microgels. (Paper IV + results from study IV not included in the paper)

Peptide cyclization

Effect of peptide cyclization on the interaction between antimicrobial peptides and oppositely charged microgels was investigated in Paper II. The studied linear and cyclic peptides were demonstrated to display random coil conformation both in aqueous solution and when bound to microgels, allowing effects of cyclization to be monitored without interference from conformational transitions. For all peptide lengths, the difference between cyclic and linear peptide variants in peptide induced microgel deswelling and electrolyte-induced peptide desorption from microgels was marginal (*Figure 20*), hence cyclization had little or no influence in peptide incorporation into, and release from, oppositely charged microgels.

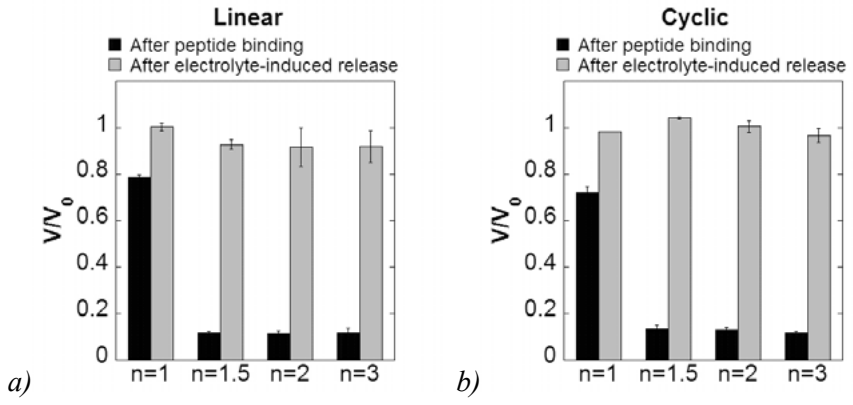

Figure 20. Final volume ratio in 20 mM ionic strength, pH 7.4, of 25% p(AAc/AAm) microgels after exposure to 5 μM linear (a) or cyclic (b) $(ARKKAAKA)_n$ with varied peptide sequence repetition (n) (black), followed by rinsing with buffer solution of 150 mM (grey). (Paper II)

Peptide secondary structure

Effects of peptide secondary structure was investigated in Paper I by incorporating antimicrobial EFK17 peptides into p(AAc/AAm) microgels of various charge densities. As shown in *Figure 21* for 50% p(AAc/AAm) microgels, peptide binding is highly influenced by peptide secondary structure. In particular, peptide uptake into the microgel increases in response to the formation of an amphiphilic helix in the peptide. Thus, EFK17-a displays a pronounced α-helix induction on peptide binding to the microgels, resulting in a correspondingly high peptide uptake and high peptide-induced microgel deswelling. EFK17-d/a, on the other hand, a peptide variant containing four d-amino acid substitutions, having identical composition and sequence as EFK17-a, but lacking the ability of α-helix formation, shows a significant reduction in both peptide uptake and peptide-induced microgel deswelling, demonstrating that conformational effects (at least those resulting in the formation of highly amphiphilic structures) influence peptide-microgel interactions.

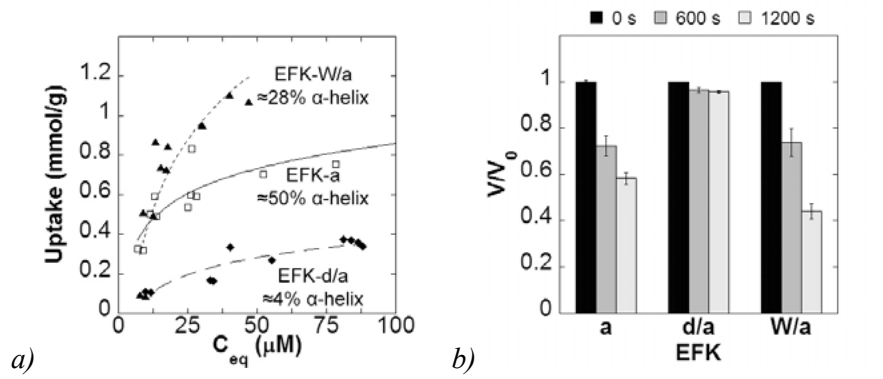

Figure 21. (a) Peptide uptake into microgels and percentage of α-helix content when bound to microgels. (b) Microgel volume ratios upon the addition of 5 μM peptide solution for three different times. Both in (a) and (b); 50% p(AAc/AAm) microgels in 10 mM ionic strength, pH 7.4. (Paper I)

For EFK17-W/a, the peptide variant containing four tryptophan substitutions, the above conformation-dependent amphiphilicity is combined with an enhanced conformation-independent amphiphilicity due to the surface active tryptophan residues. Consequently, microgel binding for EFK17-W/a, and the resulting microgel deswelling, is higher than that for both EFK17-a and EFK17-d/a (*Figure 21*).

Effect of microgel charge density

Interactions between peptides and microgel do not solely depend on peptide characteristics; of course microgel properties constitute a major role in these relations as well. In the studies performed in this thesis, focus was placed on effect of microgel charge density by varying the amount of AAc in p(AAc/AAm) microgels, together with effects of ionic strength and pH. It has previously been shown, by for example potentiometric and conductometric titration, that the swelling/deswelling of the studied p(AAc/AAm) microgels is completely reversible on pH and ionic strength variations (for peptide void microgels). Furthermore, the charge content of these microgels has been shown to increase linearly with the AAc monomer ratio, enabling charge density correlations to be drawn when comparing microgels with varied amount of AAc.[60, 86]

In *Figure 22*, it is demonstrated that the peptide-induced microgel deswelling is more pronounced for the 50% p(AAc/AAm) microgel compared to the 25% charged gel. In addition, CLSM images and intensity measurements show that more oppositely charged peptide is bound to the higher charged microgel compared to the lower charged one. These results are in agreement with former findings on the effect of charge contrast on peptide

binding to oppositely charged microgels.[60] In addition, it was previously shown, both for pAAc, PNIPAM, and starch microgels, that peptide/protein uptake increases with increasing microgel charge density due to the higher uptake capacity of microgels containing more charged residues.[60, 87, 88]

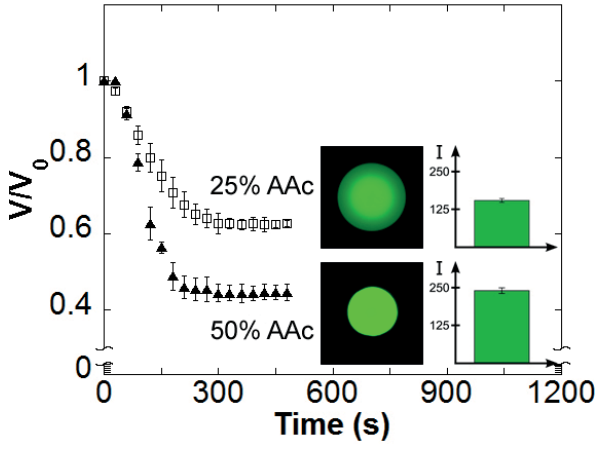

Figure 22. Peptide-induce microgel deswelling kinetics at increasing microgel charge density for p(AAc/AAm) microgels and 10 kDa pLys at 150 mM ionic strength, pH 7.4. The CLSM images and diagrams in the inset display the distribution of bound peptide and the mean peptide intensity (I), respectively. (Paper IV + results from study IV not included in the paper)

For the EFK17 peptide variants, the effect of microgel charge density is best clarified by the electrolyte-induced peptide desorption for EFK-W/a. In *Figure 23 a*, a decreased peptide desorption with increasing microgel charge density can be seen. Furthermore, as demonstrated for EFK-W/a in *Figure 23 a*, almost no electrolyte-induced peptide desorption is seen for the highest charge density. The same phenomenon can be seen in *Figure 23 b*, where the charge density dependency is demonstrated for the longest peptide variant studied in Paper II. Again, a correlation between the charge density and electrolyte-induced peptide desorption can be seen, where an increased microgel charge density results in a decreased peptide desorption.

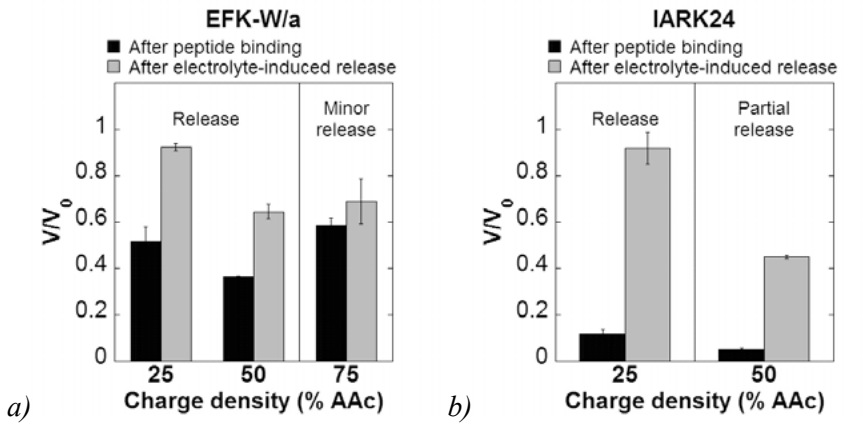

Figure 23. Final volume ratio in 10 (a) and 20 mM (b) ionic strength, pH 7.4, of p(AAc/AAm) microgels of various charge densities after exposure to 5 μM of EFK-W/a (a; Paper I) or lARK24 (b; Paper II) (black), followed by a buffer solution of 150 mM (grey).

Ionic strength and pH dependence

By changing the ionic strength or pH, peptide-microgel interactions are altered. As demonstrated in *Figure 17* for lysine oligopeptides, increasing the ionic strength reduces the peptide binding to the microgel network and the resulting peptide-induced microgel deswelling. This phenomenon is utilized in Paper I-II as demonstrated in, for example, *Figure 23 b*. In this case the peptide lARK24 is completely released from the lowest charged microgel when exposed to 150 mM ionic strength, demonstrated by complete microgel re-swelling. A similar correlation was previously shown for negatively charged starch microgels adsorbing positively charged lysozyme, where a screened electrostatic attraction between lysozyme and microgel was seen with increasing ionic strength, resulting in reduced adsorption and increased lysozyme release rate.[89]

The charge density of both pAAc and lysine oligomer is dependent on pH. Lysine oligomers are highly charged at both pH 8 and 5 whereas pAAc is fully charged at pH 8 but show a lower charge density at pH 5.[81] In *Figure 17* it can be seen that a decrease in microgel charge density by a decreased pH induces increased peptide-induced microgel deswelling. This is a result of the low charge content of the microgel at the lower pH and consequently a decreased number of charges that needs to be neutralized in order for the peptide to completely collapse the microgel network. These results are in line with previously results on larger pLys homopolypeptides and pAAc microgels.[79]

In order to further describe the systems in Paper III, a model was developed, in which counterion/peptide-mediated electrostatic attraction between the network chains is described. The model was demonstrated to be able to

capture this pH- and electrolyte-dependent microgel swelling/deswelling behavior.

Peptide distribution

Whether a peptide distributes evenly throughout the microgel or displays surface distribution/shell formation depends on the interactions at hand. Surface distributions take place when microgel deswelling on peptide incorporation is sufficiently extensive and fast to hinder continued peptide diffusion toward the microgel center. This fast surface deswelling could be due to low microgel charge density/swelling prior to peptide addition, to large charge contrast between peptide and microgel, or to presence of hydrophobic interactions. As shown in *Figure 19*, there is also a correlation between peptide molecular weight and peptide distribution. The higher the peptide molecular weight, the more susceptible it is to surface confinement. The shell formation demonstrated for the largest peptide molecular weight, and the core distribution demonstrated for the smallest molecular weight, is in line with previously results for high molecular weight peptides.[79, 81, 90]

Also for small peptides, shell formation occurs for peptides strongly interacting with oppositely charged microgels. For example, *Figure 24* demonstrates, for EFK-W/a, that microgel shell-formation and wrinkling is dependent on the charge contrast between microgel and peptide. Thus, low charge contrast at 25% p(AAc/AAm) microgels induces shell formation but no wrinkling whereas, at high charge contrast, for 75% p(AAc/AAm) microgels, shell formation is more pronounced, with additional wrinkling.

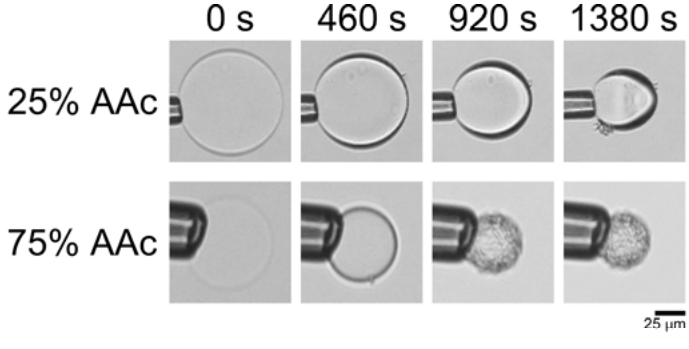

Figure 24. Exemplifying light microscopy images showing time-dependent shell formation and wrinkling upon binding of 5 µM EFK-W/a to 25% and 75% p(AAc/AAm) microgels in 10 mM ionic strength, pH 7.4. (Paper I)

Peptide degradation

To be able to use microgels as delivery systems for proteins and peptides, not only effect of peptide binding, distribution, and release from microgels need to be investigated. If used as delivery systems, microgels are exposed to enzymes and hence, also factors determining enzymatic degradation of microgel-bound peptides need to be clarified. Therefore, in Paper IV, microgel charge density, peptide length, and enzyme concentration were investigated regarding their effect on peptide degradation and release in/from microgels.

Enzyme concentration effects

Proteolytic degradation and release of microgel-bound peptides depends on the enzyme concentration. Thus, an increased enzyme concentration accelerates degradation and induces a faster microgel re-swelling time in response to degradation (*Figure 25*). From CLSM analysis in *Figure 26*, it is confirmed that microgel re-swelling corresponds to a decreased amount of microgel-bound peptide; furthermore, full microgel re-swelling corresponds to complete peptide degradation/release. As the peptide concentration inside the microgel decreases, osmotic pressure drives water uptake, resulting in microgel re-swelling.

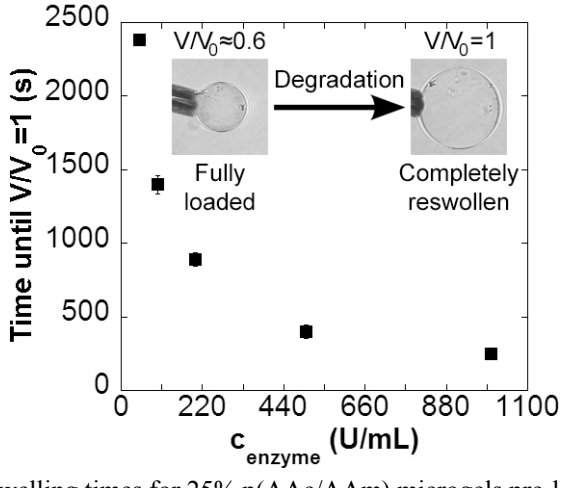

Figure 25. Re-swelling times for 25% p(AAc/AAm) microgels pre-loaded with 10 kDa pLys, as a response to enzyme exposure at varied trypsin concentrations in 150 mM ionic strength, pH 7.4. Time until V/V_0=1 corresponds to complete microgel re-swelling due to total peptide degradation/release. The inset displays exemplifying microscopy images of a microgel after peptide binding and after complete peptide degradation. (Paper IV)

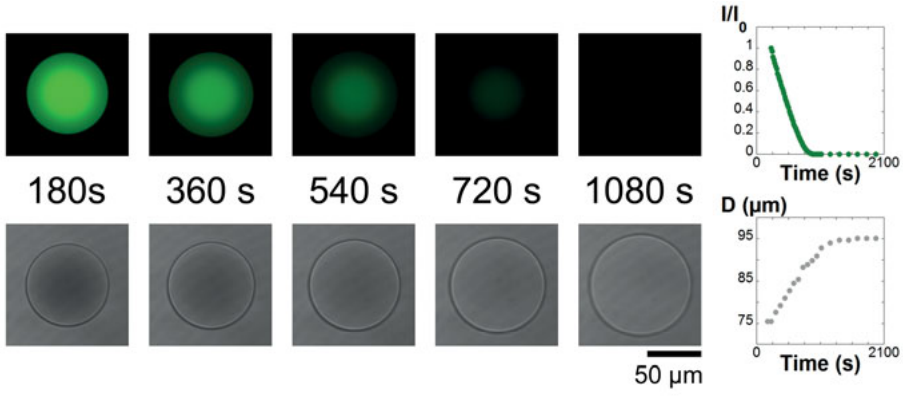

Figure 26. CLSM images displaying the degradation of 10 kDa Alexa488-pLys in 25% p(AAc/AAm) microgels due to exposure of 100 U/mL of trypsin solution in 150 mM ionic strength, pH 8.3. Top and bottom right diagrams display the relative intensity (I/I_0) of Alexa488-pLys and microgel diameter (D), respectively. (Paper IV)

Peptide length effects

Enzyme-induced microgel re-swelling due to peptide degradation is dependent on the peptide molecular weight as shown in *Figure 27*. Increased peptide length results in longer time needed to reach complete degradation and subsequent release of microgel-bound peptides. Thus, degradation of microgel-bound pLys proceeds until only lysine segments shorter than the critical desorption length remains and all lysine segments are released. With increasing peptide molecular weight, longer degradation time (and/or higher enzyme concentrations) is evidently needed until only these short peptide fragments remain and all peptide is released and the microgel fully re-swollen. Furthermore, in Paper IV, this experimentally observed peptide molecular weight dependence, together with effect of enzyme concentration, was demonstrated to be able to be qualitatively described with a simple random scission model.

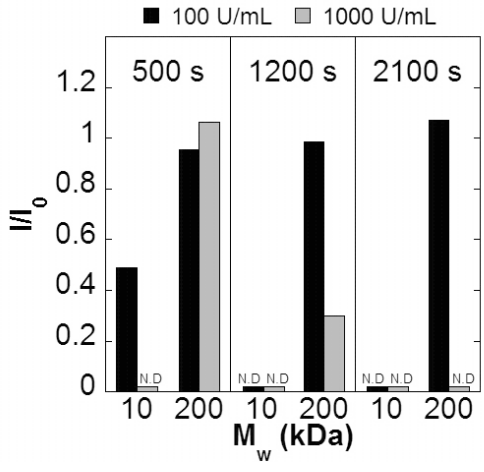

Figure 27. Relative intensity (I/I_0) from CLSM measurements displaying the degradation of Alexa488-pLys, of varied molecular weight, in 25% p(AAc/AAm) microgels at 150 mM ionic strength, pH 8.3, for three different times. Two trypsin concentrations are shown; 100 (black) and 1000 U/mL (grey). N.D. refers to non-detectable intensity, corresponding to complete peptide degradation/release. (Paper IV)

Microgel charge density effects

As demonstrated in *Figure 28*, enzyme-induced microgel re-swelling decreases with increasing microgel charge density. For the two highest charge densities, 75 and 100%, no degradation-induced peptide desorption is detected, not even at longer times (Paper IV). Consequently, at these high charge densities, the microgel-bound peptide is protected against proteolytic degradation. As discussed previously, electrostatic interactions increases with charge contrast between microgel-peptide, resulting in an increased peptide binding affinity and a tighter network (and a more pronounced microgel deswelling, as demonstrated in *Figure 28* and *Figure 22*). Due to increased network tightness, enzyme access capability to the entire peptide-loaded microgel network is decreased with an increased microgel charge density. Additionally, the inset in *Figure 22* demonstrates that more peptide is bound to the higher charged microgel, confirmed by increased mean peptide intensity. Subsequently, another contribution to the decreased degradation-induced re-swelling kinetics observed with increased microgel charge density could be that a longer time is required to degrade the larger amount of bound peptide.

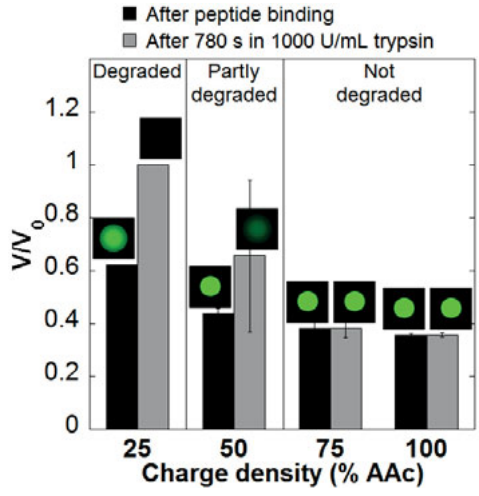

Figure 28. Volume ratios in 150 mM ionic strength, pH 7.4, of p(AAc/AAm) microgels of various charge densities after exposure to 5 µM 10 kDa pLys (black), followed by 780 s in 1000 U/mL trypsin solution (grey). The insets display demonstrative CLSM images of pLys in microgels. (Paper IV)

Matrix degradation

Shifting perspective from the non-degrading p(AAc/AAm) microgels to a more application-oriented system with a degrading matrix, Paper V focuses on effects of protein loading on the degradation of the polymer matrix in biodegradable dextran microgels. In the chosen system, microgel-peptide interactions are not driven by electrostatics, instead a high binding affinity between microgel-peptide is accomplished by a carbohydrate binding protein in combination with a carbohydrate matrix. By this, distinct effects of matrix blocking by bound protein are obtained, together with possibilities for competitive release by addition of glucose, which in itself does not affect the matrix network. In Paper V, effects of enzyme, protein, and glucose concentration were investigating regarding their effect on microgel matrix degradation.

Enzyme concentration effects

Enzymatic degradation of dextran-based microgels by dextranase is dose-dependent, as seen in *Figure 29 a*. An increased enzyme concentration induces a decreased degradation time, especially clear for protein void microgels. It has previously been clarified that the degradation of dextran-based macrogels depends on the relative enzyme amount.[68, 73, 74] In Paper V, it was elucidated that this is true also for microgels. The degradation process of the

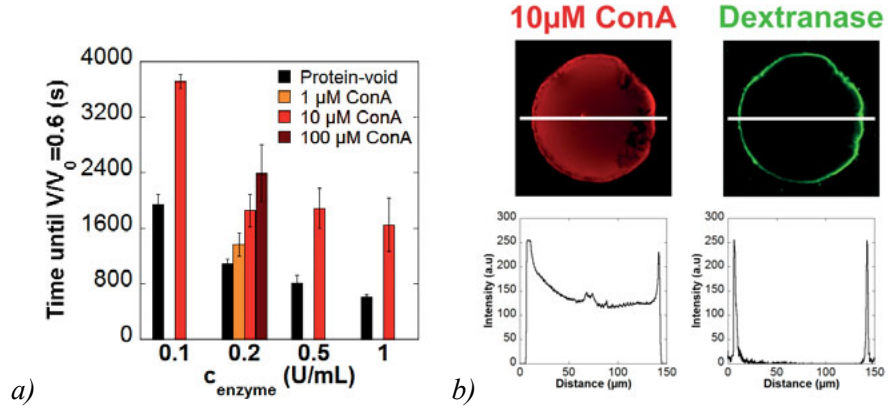

Figure 29. (a) Enzymatic degradation of protein-void and protein-loaded (1, 10, or 100 μM ConA) dextran microgels as a response to enzyme exposure at varied dextranase concentrations, in 10 mM ionic strength, pH 7.4. Time until V/V_0=0.6 corresponds to close to complete microgel disintegration. (b) ConA-Alexa633 (10 μM) and dextranase-Alexa488 (100 U/mL) distribution in microgels at 10 min after mixing, from CLSM experiments. (Paper V)

system, as demonstrated in *Figure 30*, is a combination of surface and bulk erosion, however, with surface erosion as the main mechanism. As displayed in *Figure 30*, the microgel becomes gradually more diffuse when exposed to the enzyme, indicating some bulk erosion. It is even clearer, however, that the microgel volume decreases during degradation, indicating that the degradation is particularly important at the surface. The CLSM figures and intensity profiles in *Figure 29 b* further demonstrate that surface erosion is the main degradation mechanism, especially for protein-loaded microgels, where the enzyme displays distinct surface localization. The demonstrated degradation mechanism is expected due to the relatively large size of dextranase (Table 2). This erosion mechanism is in line with previously results, showing surface degradation to be the main process for dextran methacrylate microgels.[63]

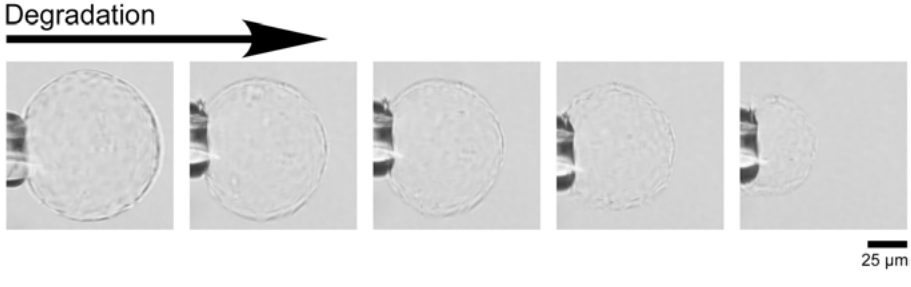

Figure 30. Exemplifying light microscopy images of a protein-void dextran microgel from different stages of the degradation, upon the addition of 0.2 U/mL dextranase in 10 mM ionic strength, pH 7.4. (Paper V)

Protein concentration effects

An increased ConA concentration results in an increased protein load in microgels, as demonstrated by CLSM measurements in *Figure 31 a*. As a consequence, microgel degradation decreases with an increased protein load (*Figure 29 a* and *Figure 31 b*), suggesting that bound ConA protects the dextran chain in the microgel matrix from enzymatic degradation through substrate access limitations. In addition, incorporation of ConA in dextran hydrogels has previously been shown to result in a tighter network structure due to induced carbohydrate linkages by the tetravalent sugar binding ConA,[91] further restricting dextranase substrate access, resulting in a decreased degradation. Addressing the relative importance of these effects, comparison of microgel degradation to that of non-cross-linked dextran, *Figure 31 b*, reveals that a significantly smaller obstruction by ConA can be seen for non-cross-linked dextran. These results demonstrate that ConA limits enzyme substrate access in dextran microgels primarily through pore blocking and induction of pore shrinkage.

Above experimentally observed effects of ConA chain blocking, together with enzyme concentration effects, was in addition, in Paper V, qualitatively described with a modified Michaelis-Menten approach for spherical symmetry, in which network blocking by ConA was included.

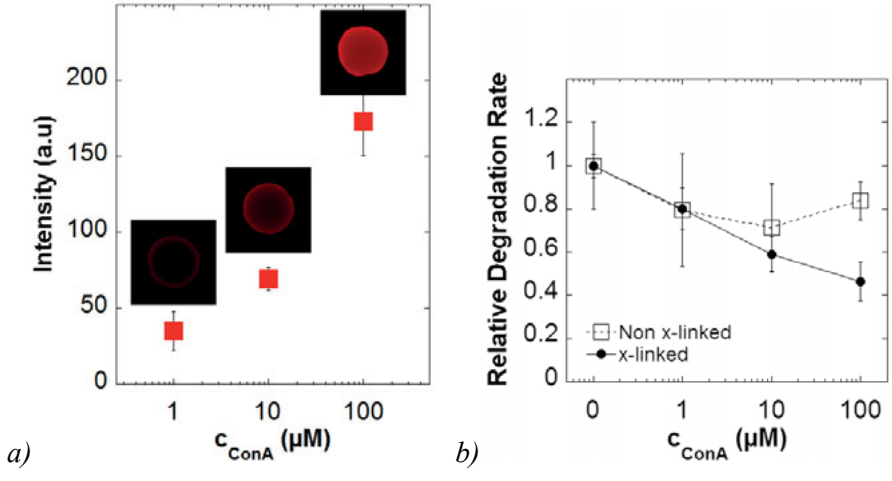

Figure 31. (a) Effect of ConA concentration on the mean fluorescence intensity from ConA-Alexa633-bound to dextran microgels in 10 mM ionic strength, pH 7.4. The insets display CLSM images, demonstrating the amount protein bound at each ConA concentration. (b) Comparison of dextranase degradation of dextran microgels with that of non-cross-linked dextran (for 0.2 U/mL dextranase). The relative degradation rate was obtained by normalizing the degradation rate (The degradation rate is set equivalent to the degree of activity and to the inverted time to reach V/V_0=0.6 for non-cross-linked and cross-linked, respectively) with that in the absence of Con A. (Paper V)

Glucose competitiveness

D-glucose can be used for competitive displacement of dextran-bound ConA due to its higher binding affinity for glucose than for dextran.[92-95] As a result of this, an increased glucose concentration induces ConA desorption and an increased enzymatic degradation of ConA-loaded microgels (*Figure 32 a*). At sufficiently high glucose concentrations, the time until complete microgel disintegration approaches that of protein-void microgels. Moreover, the CLSM measurements displayed in *Figure 32 b*, elucidate that microgel-bound ConA is completely released at sufficient high glucose concentrations.

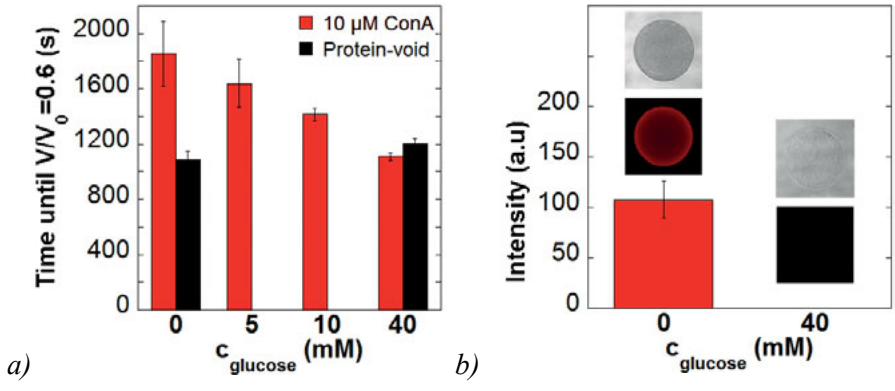

Figure 32. (a) Enzymatic degradation of protein-loaded (10 µM ConA) and protein-void dextran microgels in response to dextranase exposure (0.2 U/mL) in absence and presence of glucose of various concentrations, in 10 mM ionic strength, pH 7.4. Time until V/V_0=0.6 corresponds to close to complete microgel disintegration. (b) CLSM measurements displaying ConA-Alexa633 (10 µM) mean intensity (bar graph) and distribution (images) in microgels after equilibrating with either 0 or 40 mM glucose solution for 30 min. For 40 mM glucose solution, no intensity was detected. (Paper V)

Conclusions

The results presented in this thesis demonstrate that microgel deswelling kinetics and matrix degradation, along with peptide/protein distribution and release due to screened electrostatics, or to degradation, are dependent on a number of parameters. These include microgel charge density, peptide-length, -charge, and –charge density, peptide secondary structure and cyclization, as well as the concentration of both peptide and enzyme. By tuning these parameters, controlled peptide loading and release can be achieved, of interest for the use of microgels in protein/peptide drug delivery, as well as in related biomedical applications.

Specifically, the results presented show that peptide incorporation and peptide-induced microgel deswelling increases with peptide length (both for cyclic and linear peptide variants) and with peptide charge density. In addition, peptide charge (length) rather than peptide charge density, determines microgel deswelling. Surface distribution may occur for longer peptides, whereas shorter peptides displayed a more homogeneously core distribution, except if peptide-microgel interactions are highly attractive. In addition, peptide secondary structure, hydrophobic interactions, and microgel-peptide charge contrast all influence microgel deswelling kinetics.

Comparison between cyclic and linear peptide variants displayed marginal or no difference, indicating that end-to-end cyclization has little or no influence on peptide binding to oppositely charged microgels or on peptide-induced microgel deswelling. Cyclic and linear peptide variants also displayed similar electrolyte-induced peptide desorption from microgels. Hence, end-to-end cyclization does not noticeably influence peptide-microgel interactions, suggesting that peptide cyclization can be used in combination with oppositely charged microgel carriers to improve the proteolytic and chemical stability of the peptide compared to the corresponding linear variant.

In addition, peptide microgel binding and resulting microgel deswelling increases with the formation of an amphiphilic helix in the peptide, demonstrating that peptide binding to microgel is highly influenced by peptide secondary structure. An increased peptide binding and microgel deswelling was also shown for the peptide modified with selected tryptophan substitutions, indicating the importance of both conformation-dependent and -independent amphiphilicity effects for this peptide variant.

With respect to ambient conditions, microgel deswelling was demonstrated to be promoted at lower pH. In addition, reducing the electrostatic interactions by increasing the ionic strength was shown to induce peptide release. Here, decreased peptide desorption was seen with increased microgel charge density and/or with increased peptide length.

The enzymatic degradation of peptide incorporated into microgels of oppositely charge increases with increasing enzyme concentration, decreased microgel charge density, and decreased peptide molecular weight. Consequently, all these factors influence microgel-bound peptide degradation. Of importance for applications, protective effects of microgels against proteolytic peptide degradation were observed only at sufficiently high microgel charge density.

Enzyme-mediated microgel degradation was shown to increase with increasing enzyme concentration, while an increased protein loading in microgels caused a concentration-dependent decrease in microgel degradation. The outer region of the microgel was shown to be continuously degraded on enzyme exposure, resulting in a microgel volume decrease. Comparison of microgel degradation to that of non-cross-linked dextran demonstrated that ConA limits enzyme substrate access in dextran microgels primarily through pore blocking and induction of pore shrinkage. In addition, in the presence of glucose, competitive release of microgel-bound sugar-binding protein was demonstrated to restore the microgel degradation observed in the absence of the protein.

Taken together, results presented in this thesis have provided some insight on factors of importance for loading and release of proteins or peptides in microgels, of interest for the use of microgels as delivery systems for peptide and protein drugs. For example, results presented herein clarify that there is an important interplay between microgel and peptide/protein for their respective biodegradation, of obvious importance for drug delivery, but also in a host of other biomedical applications.

Development outlook

The first reported preparation of microgels is about 80 years ago by the discovery of Staudinger and Husemann,[96] however, the term microgel was first introduced by Baker more than ten years later.[6, 97] Since then, knowledge of microgels has significantly progressed, but there are still needs for further developments before microgels can be fully utilized for biomedical applications. For example, it is essential that microgels are prepared from monomers and other components which are biocompatible, and ideally already approved for use in pharmaceuticals or medical devices. Biodegradability is another aspect requiring further attention in order to ensure controlled degradation/removal of the microgels from the body after completing their mission, to be able to avoid surgical procedure. Another issue that needs to be considered for microgels is their size. Depending on the intended application, different microgel dimensions are desired. For example, in intravenous drug delivery, it has been concluded that the preferable nanoparticle size range is around 10 to 100 nm.[14] In addition, microgel size variations influence the bioavailability as well as the blood circulating time if used in drug delivery, and therefore, microgels should be aimed at being synthesized with a narrow size distribution.[14, 98, 99]

Overall, the outlook for microgels in biomedical applications, especially as drug delivery vehicles, is good. The high water content of microgels, mechanical similarities with soft human tissue (such as connective tissues, ligaments, blood vessels etc.), and possibility for good biocompatibility, in addition to their capability to incorporate and protect biomacromolecular drugs and to release these in response to a variety of triggering parameters, suggest microgels to provide interesting opportunities within biomedical applications such as in drug delivery, functional biomaterials, regenerative medicine, and biosensors.

Populärvetenskaplig sammanfattning

Mikrogelers växelverkan med peptider och proteiner

Konsekvens av peptiders och mikrogelers egenskaper

Framsteg inom molekylär- och cellbiologi har under senare år lett till utvecklingen av ett brett utbud av nya biologiska aktiva makromolekyler, såsom protein- och peptidläkemedel, för behandling av mänskliga sjukdomar. En utmaning är dock att få en effektiv leverans av dessa läkemedel till platsen där de ska ge sin verkan. Detta försvåras av proteiners och peptiders känslighet mot aggregering och konformationsförändringar, samt mot kemisk och enzymatisk nedbrytning, vilket leder till att de förlorar sin aktivitet. För att uppnå en önskvärd terapeutisk effekt och för att nå en bredare terapeutisk tillämpning för dessa läkemedel krävs därför att nya läkemedelsbärare utvecklas. Dessa läkemedelsbärare måste vara kapabla att kapsla in och skydda inkorporerade läkemedel, och skall dessutom möjliggöra kontrollerad läkemedelsfrisättning. Ett tillvägagångssätt för att kapsla in och skydda biologiskt aktiva protein- och peptidläkemedel är att använda sig av mikrogeler.

Mikrogeler är sfäriska partiklar, med en medeldiameter mellan 10 nm och 100 µm, som består av ett tredimensionellt nätverk av löst tvärbundna polymerer som är svällda med vatten. Dessa nätverk har en förmåga att krympa och svälla i hög grad som respons på förändringar i den omgivande lösningen. Inbindning av peptider och proteiner till mikrogeler kan ske på grund av elektrostatiska interaktioner mellan peptid och mikrogelens nätverk, om de respektive komponenterna har motsatt laddning. När peptider binder in till mikrogeler genom elektrostatisk attraktion kommer mikrogelens nätverk att dra ihop sig och mikrogelen krymper, vilket resulterar i att mikrogelen effektivt kan skydda den inbundna peptiden. Inbunden peptid kan sedan frisättas genom att de elektrostatiska attraktionerna minskas genom till exempel en ökad salthalt. Mikrogeler kan även designas för att vara känsliga för en annan parameter är salthalt, såsom temperaturändringar, närvaro av specifika metaboliter, och nedbrytning. En stor fördel med att använda mikrogeler som bärarsystem för peptid- och proteinläkemedel är att en kontrollerad läkemedelsfrisättningshastighet kan uppnås. Dessutom erbjuder mikrogeler en rad fördelar för de inbundna protein- och peptidläkemedlen, såsom behållning av sekundär och tertiär struktur, skydd mot aggregering och mot enzy-

matisk och kemisk nedbrytning. Detta resulterar i att läkemedlets biologiska aktivitet bibehålls, i en minskad toxicitet och immungenicitet, samt i en reducering av andra biologiska biverkningar.

Målsättningen med denna avhandling är att klargöra några av de viktigaste faktorer som påverkar peptiders inbindning i, distribution inom, och frisättning från mikrogeler. Dessutom syftar avhandlingen till att undersöka hur dessa faktorer påverkas av egenskaper hos såväl peptiden som hos mikrogelen. Utöver detta avser avhandlingen att även utreda de parametrar som påverkar proteolytisk nedbrytning av peptider inbundna i mikrogeler samt de parametrar som påverkar proteolytisk nedbrytning av själva nätverket i mikrogelen, både i närvaro och i frånvaro av inbunden peptid/protein.

Resultaten visar att mängden inbunden peptid, såväl som peptidinducerad krympning av mikrogeler, ökar med peptidernas längd och laddningsdensitet. Dessutom påverkar peptidernas laddning (längd), snarare än laddningsdensitet, mikrogelers krympning. Cyklisering av peptider påverkar inte märkbart interaktionerna mellan peptid och mikrogel, vilket visar att cyklisering av peptider kan användas i kombination med mikrogeler för att förstärka peptidens proteolytiska och kemiska stabilitet jämfört med motsvarande linjära variant. Det demonstreras även att sekundärstrukturen kraftigt påverkar peptidernas inbindning i, och frisättning från, mikrogeler. Vidare visas det att mikrogelens laddningsdensitet, peptidernas molekylvikt och koncentrationen av enzym har en stark inverkan på nedbrytningen av inbunden peptid. En tillräckligt skyddande effekt mot nedbrytning av inbunden peptid observeras endast för tillräckligt hög laddningsdensitet hos mikrogelerna. Det visas även, för nedbrytningsbara mikrogeler, att nedbrytning av mikrogelens nätverk ökar med ökande enzymkoncentration. Däremot orsakar en ökad inbindning av protein i mikrogeler en koncentrationsberoende minskning av den enzymatiska nedbrytningen av mikrogelernas nätverk.

Sammanfattningsvis har resultat erhållna i avhandlingen bidragit till kunskapen om faktorer av betydelse för en ändamålsenlig användning av mikrogeler som läkemedelsbärare för protein- och/eller peptidläkemedel. Presenterade resultat visar tydligt på ett samspel mellan mikrogel och peptid/protein vilket är av betydelse för deras respektive biologiska nedbrytning och av tydlig relevans för kontrollerad läkemedelstransport och frisättning, samt för en mängd andra biomedicinska tillämpningar såsom biomaterial och regenerativ medicin.

Acknowledgements

The work in this thesis was carried out at the Department of Pharmacy, Faculty of Pharmacy, Uppsala University, Sweden. The studies were financially supported by the Swedish Research Council.

I gratefully acknowledge travel grants from Apotekarsocieteten (*Elisabeth och Alfred Ahlqvists stiftelse* and *Apotekare C.D Carlssons stiftelse*) that made it possible for me to participate at international research conferences.

I would like to express my sincere gratitude to all of you who made this work possible:

Min handledare *Martin Malmsten*, för att du delat med dig av din omfattande expertis inom området. Jag vill även tacka dig för en mycket effektiv handledning och för de extremt snabba svaren på alla mail, dygnet runt! Sover du aldrig?

Min biträdande handledare *Per Hansson*, för att du alltid med ett glatt humör tagit dig tid att hjälpa mig hitta svar på diverse funderingar och tankar.

People in *Prof. Brian Vincent* group, at the School of Chemistry, University of Bristol, especially *Dr. Melanie Bradley,* for being a great "supervisor" and teaching me all about gel synthesis.

Stort tack till alla gamla och nuvarande kollegor i *fysikalgruppen*. Jag vill särskilt uppmärksamma:

Lotta, min "Uppsalamormor", för din omtanke och kärlek. För att du alltid finns tillgänglig, både i glada och jobbiga stunder. Jag kommer sakna dig. Förresten Lotta, jag måste erkänna, den där skylten utanför ditt kontor, det är jag som är skyldig… hihi☺

Anders, för att du lät mig vara din "Deputy Sheriff"! Stort tack för att du alltid lyssnat på mina tankar och idéer kring undervisning och framförallt för att jag faktiskt har fått utföra de förändringar jag haft på förslag. Sen du gick i pension har undervisningen inte varit lika glädjefylld och givande.

Birgitta, för ditt stöd under åren och för den trygghet och ro du tillfört i gruppen. Det blev ett stort hål när du gick i pension, jag saknar dig.

Helena, för att du lärde mig ”allt du kunde” och för att du svarat på de många frågor och funderingar jag haft under åren. Du är en förebild!

Shalini, for good companionship at conferences and courses. For patiently following me on all of my long shopping trips in USA and for all the nice dinners we enjoyed!

Lina och *Randi*, för att ni alltid har humöret på topp och för era glada skratt som ekar i labbet☺

Maria and *Pia*, for your undergraduate projects and nice collaborations.

Jonas, *Martin A* och *Claes*, se nu till att inte stöka till det allt för mycket på de labb ni jobbar i framtiden... Ordning och reda, städning på fredag!

Min medförfattare *Göran*, tack för att du bidragit med de kunskaper jag saknat och tack för ett trevligt samarbete.

Alla nuvarande och tidigare *doktorander* på institutionen ska ha ett stort tack för alla trevliga fika, luncher och andra tillställningar!

Jag vill tacka *Annette Svensson Lindgren*, *Eva Nises-Ahlgren* och *Ulla Wästberg-Galik* för all administrativ hjälp genom åren.

Anneli, tack för alla långa luncher där vi pratat om allt mellan himmel och jord. Du är verkligen en genomgod person och jag är så glad att jag fått chansen att lära känna dig, vilken tur att vi ”klickade” i Parma!

~

Mina *Svärföräldrar*, tack för att ni låter mig vara en del av er familj och för att ni stöttat oss i vårt beslut att flytta till Uppsala. Det betyder mycket för mig!

Mamma och *Pappa*, tack för att ni alltid uppmuntrat och stöttat mig, vad jag än har fått för mig. Den trygghet som ni ger mig betyder väldigt mycket för mig. Älskar er!

Emil, utan dig hade den här resan varit omöjlig. Det stöd du gett mig under dessa år är något jag aldrig kommer att glömma. Det är du som gett mig kraft och styrka att klara av det här. Du är min sol. Mitt hjärta är ditt. Jag älskar dig♥

References

1. Bysell, H., Mansson, R., Hansson, P., and Malmsten, M. *Microgels and microcapsules in peptide and protein drug delivery.* Adv. Drug Delivery Rev. **2011**, *63*, 1172-1185.
2. Langer, R. *New Methods of Drug Delivery.* Science **1990**, *249*, 1527-1533.
3. Malmsten, M., Bysell, H., and Hansson, P. *Biomacromolecules in microgels - Opportunities and challenges for drug delivery.* Curr. Opin. Colloid Interface Sci. **2010**, *15*, 435-444.
4. Pich, A. and Richtering, W. *Microgels by Precipitation Polymerization: Synthesis, Characterization, and Functionalization. Chemical Design of Responsive Microgels.* Adv. Polym. Sci. **2010**, *234*, 1-37.
5. Oh, J.K., Drumright, R., Siegwart, D.J., and Matyjaszewski, K. *The development of microgels/nanogels for drug delivery applications.* Prog. Polym. Sci. **2008**, *33*, 448-477.
6. Saunders, B.R., Laajam, N., Daly, E., Teow, S., Hu, X., and Stepto, R. *Microgels: From responsive polymer colloids to biomaterials.* Adv. Colloid Interface Sci. **2009**, *147-148*, 251-262.
7. Nayak, S. and Lyon, L.A. *Soft nanotechnology with soft nanoparticles.* Angew. Chem., Int. Ed. **2005**, *44*, 7686-7708.
8. Malmsten, M. *Soft drug delivery systems.* Soft Matter **2006**, *2*, 760-769.
9. Frokjaer, S. and Otzen, D.E. *Protein drug stability: A formulation challenge.* Nat. Rev. Drug Discovery **2005**, *4*, 298-306.
10. Young, S., Wong, M., Tabata, Y., and Mikos, A.G. *Gelatin as a delivery vehicle for the controlled release of bioactive molecules.* J. Controlled Release **2005**, *109*, 256-274.
11. Maulding, H.V. *Prolonged Delivery of Peptides by Microcapsules.* J. Controlled Release **1987**, *6*, 167-176.
12. Pean, J.M., Venier-Julienne, M.C., Boury, F., Menei, P., Denizot, B., and Benoit, J.P. *NGF release from poly(D,L-lactide-co-glycolide) microspheres. Effect of some formulation parameters on encapsulated NGF stability.* J. Controlled Release **1998**, *56*, 175-187.
13. Crotts, G., Sah, H., and Park, T.G. *Adsorption determines in-vitro protein release rate from biodegradable microspheres: Quantitative analysis of surface area during degradation.* J. Controlled Release **1997**, *47*, 101-111.
14. Vinogradov, S.V., Bronich, T.K., and Kabanov, A.V. *Nanosized cationic hydrogels for drug delivery: preparation, properties and interactions with cells.* Adv. Drug Delivery Rev. **2002**, *54*, 135-147.
15. Cerroni, B., Chiessi, E., Margheritelli, S., Oddo, L., and Paradossi, G. *Polymer Shelled Microparticles for a Targeted Doxorubicin Delivery in Cancer Therapy.* Biomacromolecules **2011**, *12*, 593-601.

16. Vinogradov, S.V. *Colloidal microgels in drug delivery applications.* Curr. Pharm. Des. **2006**, *12*, 4703-12.
17. Lam, P.L. and Gambari, R. *Advanced progress of microencapsulation technologies: In vivo and in vitro models for studying oral and transdermal drug deliveries.* J. Controlled Release **2014**, *178*, 25-45.
18. Zhang, J.F., Chen, D.D., Li, Y., and Sun, J.Q. *Layer-by-layer assembled highly adhesive microgel films.* Polymer **2013**, *54*, 4220-4226.
19. Moore, K., Amos, J., Davis, J., Gourdie, R., and Potts, J.D. *Characterization of Polymeric Microcapsules Containing a Low Molecular Weight Peptide for Controlled Release.* Microsc. Microanal. **2013**, *19*, 213-226.
20. Schmidtchen, A., Pasupuleti, M., and Malmsten, M. *Effect of hydrophobic modifications in antimicrobial peptides.* Adv. Colloid Interface Sci. **2014**, *205*, 265-274.
21. Pasupuleti, M., Schmidtchen, A., and Malmsten, M. *Antimicrobial peptides: key components of the innate immune system.* Crit. Rev. Biotechnol. **2012**, *32*, 143-171.
22. Schmidtchen, A. and Malmsten, M. *Peptide interactions with bacterial lipopolysaccharides.* Curr. Opin. Colloid Interface Sci. **2013**, *18*, 381-392.
23. Malmsten, M., *Biopolymers at Interfaces*. 2nd ed. Vol. 110. **2003**, New York: Marcel Dekker.
24. Strömstedt, A.A., Pasupuleti, M., Schmidtchen, A., and Malmsten, M. *Evaluation of strategies for improving proteolytic resistance of antimicrobial peptides by using variants of EFK17, an internal segment of LL-37.* Antimicrob. Agents Chemother. **2009**, *53*, 593-602.
25. Strömstedt, A.A., Ringstad, L., Schmidtchen, A., and Malmsten, M. *Interaction between amphiphilic peptides and phospholipid membranes.* Curr. Opin. Colloid Interface Sci. **2010**, *15*, 467-478.
26. Ovadia, O., Greenberg, S., Laufer, B., Gilon, C., Hoffman, A., and Kessler, H. *Improvement of drug-like properties of peptides: the somatostatin paradigm.* Expert Opin. Drug Discovery **2010**, *5*, 655-671.
27. Cardin, A.D. and Weintraub, H.J.R. *Molecular Modeling of Protein-Glycosaminoglycan Interactions.* Arteriosclerosis **1989**, *9*, 21-32.
28. Hoare, T.R. and Kohane, D.S. *Hydrogels in drug delivery: Progress and challenges.* Polymer **2008**, *49*, 1993-2007.
29. Schexnailder, P. and Schmidt, G. *Nanocomposite polymer hydrogels.* Colloid Polym. Sci. **2009**, *287*, 1-11.
30. Bae, K.H., Wang, L.S., and Kurisawa, M. *Injectable biodegradable hydrogels: progress and challenges.* J. Mater. Chem. B **2013**, *1*, 5371-5388.
31. Tibbitt, M.W. and Anseth, K.S. *Hydrogels as Extracellular Matrix Mimics for 3D Cell Culture.* Biotechnol. Bioeng. **2009**, *103*, 655-663.
32. Kharkar, P.M., Kiick, K.L., and Kloxin, A.M. *Designing degradable hydrogels for orthogonal control of cell microenvironments.* Chem. Soc. Rev. **2013**, *42*, 7335-7372.
33. Saxena, S., Hansen, C.E., and Lyon, L.A. *Microgel Mechanics in Biomaterial Design.* Acc. Chem. Res. **2014**, *47*, 2426-2434.

34. Pelton, R. *Temperature-sensitive aqueous microgels.* Adv. Colloid Interface Sci. **2000**, *85*, 1-33.
35. Malmsten, M. *Drugs and the Pharmaceutical Sciences. Surfactants and polymers in drug delivery.* **2002**, *122*, i-ix, 1-348.
36. Tanaka, T. and Fillmore, D.J. *Kinetics of Swelling of Gels.* J. Chem. Phys. **1979**, *70*, 1214-1218.
37. Ricka, J. and Tanaka, T. *Swelling of Ionic Gels - Quantitative Performance of the Donnan Theory.* Macromolecules **1984**, *17*, 2916-2921.
38. Lyon, L.A. and Fernandez-Nieves, A. *The Polymer/Colloid Duality of Microgel Suspensions.* Annu. Rev. Phys. Chem. **2012**, *63*, 25-43.
39. Saunders, B. and Vincent, B. *Microgel particles as model colloids: theory, properties and applications.* Adv. Colloid Interface Sci. **1999**, *80*, 1-25.
40. Nolan, C.M., Gelbaum, L.T., and Lyon, L.A. *1H NMR Investigation of Thermally Triggered Insulin Release from Poly(N-isopropylacrylamide) Microgels.* Biomacromolecules **2006**, *7*, 2918-2922.
41. Tan, J.P. and Tam, K.C. *Application of drug selective electrode in the drug release study of pH-responsive microgels.* J. Controlled Release **2007**, *118*, 87-94.
42. Kim, J.J. and Park, K. *Modulated insulin delivery from glucose-sensitive hydrogel dosage forms.* J. Controlled Release **2001**, *77*, 39-47.
43. Miyata, T., Asami, N., and Uragami, T. *A reversibly antigen-responsive hydrogel.* Nature **1999**, *399*, 766-9.
44. Gorelikov, I., Field, L.M., and Kumacheva, E. *Hybrid microgels photoresponsive in the near-infrared spectral range.* J. Am. Chem. Soc. **2004**, *126*, 15938-9.
45. Murthy, N., Xu, M., Schuck, S., Kunisawa, J., Shastri, N., and Frechet, J.M. *A macromolecular delivery vehicle for protein-based vaccines: acid-degradable protein-loaded microgels.* Proc. Natl. Acad. Sci. U. S. A. **2003**, *100*, 4995-5000.
46. Islam, M.R., Lu, Z.Z., Li, X., Sarker, A.K., Hu, L., Choi, P., Li, X., Hakobyan, N., and Serpe, M.J. *Responsive polymers for analytical applications: A review.* Anal. Chim. Acta **2013**, *789*, 17-32.
47. Yin, R.X., Tong, Z., Yang, D.Z., and Nie, J. *Glucose-responsive insulin delivery microhydrogels from methacrylated dextran/concanavalin A: Preparation and in vitro release study.* Carbohydr. Polym. **2012**, *89*, 117-123.
48. Tan, J.X., Wang, X.Y., Li, H.Y., Su, X.L., Wang, L.A., Ran, L.A., Zheng, K., and Ren, G.S. *HYAL1 overexpression is correlated with the malignant behavior of human breast cancer.* Int. J. Cancer **2011**, *128*, 1303-1315.
49. Wang, Q.C., Uzunoglu, E., Wu, Y., and Libera, M. *Self-Assembled Poly(ethylene glycol)-co-Acrylic Acid Microgels to Inhibit Bacterial Colonization of Synthetic Surfaces.* ACS Appl. Mater. Interfaces **2012**, *4*, 2498-2506.
50. Wang, Q.C. and Libera, M. *Microgel-modified surfaces enhance short-term osteoblast response.* Colloids Surf., B **2014**, *118*, 202-209.
51. Williams, D.F. *On the mechanisms of biocompatibility.* Biomaterials **2008**, *29*, 2941-2953.

52. Wang, Y.X., Robertson, J.L., Spillman, W.B., and Claus, R.O. *Effects of the chemical structure and the surface properties of polymeric biomaterials on their biocompatibility.* Pharm. Res. **2004**, *21*, 1362-1373.
53. Elbert, D.L. and Hubbell, J.A. *Surface treatments of polymers for biocompatibility.* Annu. Rev. Mater. Sci. **1996**, *26*, 365-394.
54. Anderson, J.M. *Biological responses to materials.* Annu. Rev. Mater. Res. **2001**, *31*, 81-110.
55. Xu, Z.K., Nie, F.Q., Qu, C., Wan, L.S., Wu, J., and Yao, K. *Tethering poly(ethylene glycol)s to improve the surface biocompatibility of poly(acrylonitrile-co-malele acid) asymmetric membranes.* Biomaterials **2005**, *26*, 589-598.
56. Brodbeck, W.G., Shive, M.S., Colton, E., Nakayama, Y., Matsuda, T., and Anderson, J.M. *Influence of biomaterial surface chemistry on the apoptosis of adherent cells.* J. Biomed. Mater. Res. **2001**, *55*, 661-668.
57. Mahmoudi, M., Lynch, I., Ejtehadi, M.R., Monopoli, M.P., Bombelli, F.B., and Laurent, S. *Protein-Nanoparticle Interactions: Opportunities and Challenges.* Chem. Rev. **2011**, *111*, 5610-5637.
58. Walkey, C.D. and Chan, W.C.W. *Understanding and controlling the interaction of nanomaterials with proteins in a physiological environment.* Chem. Soc. Rev. **2012**, *41*, 2780-2799.
59. von Burkersroda, F., Schedl, L., and Gopferich, A. *Why degradable polymers undergo surface erosion or bulk erosion.* Biomaterials **2002**, *23*, 4221-4231.
60. Bysell, H., Hansson, P., and Malmsten, M. *Effect of Charge Density on the Interaction between Cationic Peptides and Oppositely Charged Microgels.* J. Phys. Chem. B **2010**, *114*, 7207-7215.
61. Dendukuri, D. and Doyle, P.S. *The Synthesis and Assembly of Polymeric Microparticles Using Microfluidics.* Adv. Mater. **2009**, *21*, 4071-4086.
62. Khalikova, E., Susi, P., and Korpela, T. *Microbial dextran-hydrolyzing enzymes: Fundamentals and applications.* Microbiol. Mol. Biol. Rev. **2005**, *69*, 306-325.
63. Ghugare, S.V., Chiessi, E., Cerroni, B., Telling, M.T.F., Sakai, V.G., and Paradossi, G. *Biodegradable dextran based microgels: a study on network associated water diffusion and enzymatic degradation.* Soft Matter **2012**, *8*, 2494-2502.
64. Chen, F.M., Zhao, Y.M., Wu, H., Deng, Z.H., Wang, Q.T., Zhou, W., Liu, Q., Dong, G.Y., Li, K., Wu, Z.F., and Jin, Y. *Enhancement of periodontal tissue regeneration by locally controlled delivery of insulin-like growth factor-I from dextran-co-gelatin microspheres.* J. Controlled Release **2006**, *114*, 209-222.
65. Finnegan, P.M., Brumbley, S.M., O'Shea, M.G., Nevalainen, H., and Bergquist, P.L. *Isolation and characterization of genes encoding thermoactive and thermostable dextranases from two thermotolerant soil bacteria.* Curr. Microbiol. **2004**, *49*, 327-333.
66. Koh, T.Y. and Khouw, B.T. *A Rapid Method for Assay of Dextranase.* Can. J. Biochem. **1970**, *48*, 225-227.

67. Finnegan, P.M., Brumbley, S.M., O'Shea, M.G., Nevalainen, H., and Bergquist, P.L. *Diverse dextranase genes from Paenibacillus species.* Arch. Microbiol. **2005**, *183*, 140-147.
68. Franssen, O., Vos, O.P., and Hennink, W.E. *Delayed release of a model protein from enzymatically-degrading dextran hydrogels.* J. Controlled Release **1997**, *44*, 237-245.
69. Franssen, O., van Ooijen, R.D., de Boer, D., Maes, R.A.A., and Hennink, W.E. *Enzymatic degradation of cross-linked dextrans.* Macromolecules **1999**, *32*, 2896-2902.
70. Wu, D.T., Zhang, H.B., Huang, L.J., and Hu, X.Q. *Purification and characterization of extracellular dextranase from a novel producer, Hypocrea lixii F1002, and its use in oligodextran production.* Process Biochem. **2011**, *46*, 1942-1950.
71. Larsen, C. *Dextran Prodrugs Structure and Stability in Relation to Therapeutic Activity.* Adv. Drug Delivery Rev. **1989**, *3*, 103-154.
72. Ammon, R. *Das Vorkommen Von Dextranase Im Menschlichen Gewebe.* Enzymologia **1963**, *25*, 245-251.
73. Moriyama, K. and Yui, N. *Regulated insulin release from biodegradable dextran hydrogels containing poly(ethylene glycol).* J. Controlled Release **1996**, *42*, 237-248.
74. Hennink, W.E., Franssen, O., van Dijk-Wolthuis, W.N.E., and Talsma, H. *Dextran hydrogels for the controlled release of proteins.* J. Controlled Release **1997**, *48*, 107-114.
75. Kamath, K.R. and Park, K. *Study on the Release of Invertase from Enzymatically Degradable Dextran Hydrogels.* Polym. Gels Networks **1995**, *3*, 243-254.
76. Hovgaard, L. and Brondsted, H. *Dextran Hydrogels for Colon-Specific Drug-Delivery.* J. Controlled Release **1995**, *36*, 159-166.
77. Cadee, J.A., de Groot, C.J., Jiskoot, W., den Otter, W., and Hennink, W.E. *Release of recombinant human interleukin-2 from dextran-based hydrogels.* J. Controlled Release **2002**, *78*, 1-13.
78. Johansson, C., Hansson, P., and Malmsten, M. *Mechanism of Lysozyme Uptake in Poly(acrylic acid) Microgels.* J. Phys. Chem. B **2009**, *113*, 6183-6193.
79. Bysell, H., Hansson, P., and Malmsten, M. *Transport of poly-L-lysine into oppositely charged poly(acrylic acid) microgels and its effect on gel deswelling.* J. Colloid Interface Sci. **2008**, *323*, 60-69.
80. Smith, P.K., Krohn, R.I., Hermanson, G.T., Mallia, A.K., Gartner, F.H., Provenzano, M.D., Fujimoto, E.K., Goeke, N.M., Olson, B.J., and Klenk, D.C. *Measurement of Protein Using Bicinchoninic Acid.* Anal. Biochem. **1985**, *150*, 76-85.
81. Bysell, H. and Malmsten, M. *Visualizing the interaction between poly-L-lysine and poly(acrylic acid) microgels using microscopy techniques: Effect of electrostatics and peptide size.* Langmuir **2006**, *22*, 5476-5484.
82. Greenfield, N.J. *Using circular dichroism spectra to estimate protein secondary structure.* Nat. Protoc. **2006**, *1*, 2876-2890.

83. Sjögren, H. and Ulvenlund, S. *Comparison of the helix-coil transition of a titrating polypeptide in aqueous solutions and at the air-water interface.* Biophys. Chem. **2005**, *116*, 11-21.
84. Greenfield, N. and Fasman, G.D. *Computed circular dichroism spectra for the evaluation of protein conformation.* Biochemistry **1969**, *8*, 4108-16.
85. Bysell, H., Schmidtchen, A., and Malmsten, M. *Binding and Release of Consensus Peptides by Poly(acrylic acid) Microgels.* Biomacromolecules **2009**, *10*, 2162-2168.
86. Bysell, H., Hansson, P., Schmidtchen, A., and Malmsten, M. *Effect of Hydrophobicity on the Interaction between Antimicrobial Peptides and Poly(acrylic acid) Microgels.* J. Phys. Chem. B **2010**, *114*, 1307-1313.
87. Silva, C.S.O., Baptista, R.P., Santos, A.M., Martinho, J.M.G., Cabral, J.M.S., and Taipa, M.A. *Adsorption of human IgG on to poly(N-isopropylacrylamide)-based polymer particles.* Biotechnol. Lett. **2006**, *28*, 2019-2025.
88. Li, Y., de Vries, R., Slaghek, T., Timmermans, J., Cohen Stuart, M.A., and Norde, W. *Preparation and Characterization of Oxidized Starch Polymer Microgels for Encapsulation and Controlled Release of Functional Ingredients.* Biomacromolecules **2009**, *10*, 1931-1938.
89. Li, Y., de Vries, R., Kleijn, M., Slaghek, T., Timmermans, J., Stuart, M.C., and Norde, W. *Lysozyme Uptake by Oxidized Starch Polymer Microgels.* Biomacromolecules **2010**, *11*, 1754-1762.
90. Bysell, H. and Malmsten, M. *Interactions between Homopolypeptides and Lightly Cross-Linked Microgels.* Langmuir **2009**, *25*, 522-528.
91. Tan, H.P. and Hu, X.H. *Injectable in situ forming glucose-responsive dextran-based hydrogels to deliver adipogenic factor for adipose tissue engineering.* J. Appl. Polym. Sci. **2012**, *126*, E180-E186.
92. Edelman, G.M., Cunningham, B.A., Reeke, G.N., Becker, J.W., Waxdal, M.J., and Wang, J.L. *Covalent and 3-Dimensional Structure of Concanavalin-A.* Proc. Natl. Acad. Sci. U. S. A. **1972**, *69*, 2580-2584.
93. Zhang, R., Tang, M., Bowyer, A., Eisenthal, R., and Hubble, J. *Synthesis and characterization of a D-glucose sensitive hydrogel based on CM-dextran and concanavalin A.* React. Funct. Polym. **2006**, *66*, 757-767.
94. Huang, J., Zhang, L., Liang, R.P., and Qiu, J.D. *"On-off" switchable electrochemical affinity nanobiosensor based on graphene oxide for ultrasensitive glucose sensing.* Biosens. Bioelectron. **2013**, *41*, 430-435.
95. Cella, L.N., Chen, W., Myung, N.V., and Mulchandani, A. *Single-Walled Carbon Nanotube-Based Chemiresistive Affinity Biosensors for Small Molecules: Ultrasensitive Glucose Detection.* J. Am. Chem. Soc. **2010**, *132*, 5024-5026.
96. Staudinger, H. and Husemann, E. *On highly polymeric compounds, 116(th) Announcement - On the limite swellable poly-styrene.* Ber. Dtsch. Chem. Ges. **1935**, *68*, 1618-1634.
97. Baker, W.O. *Microgel, a New Macromolecule - Relation to Sol and Gel as Structural Elements of Synthetic Rubber.* Ind. Eng. Chem. **1949**, *41*, 511-520.

98. Stolnik, S., Illum, L., and Davis, S.S. *Long Circulating Microparticulate Drug Carriers.* Adv. Drug Delivery Rev. **1995**, *16*, 195-214.
99. Kong, G., Braun, R.D., and Dewhirst, M.W. *Hyperthermia enables tumor-specific nanoparticle delivery: Effect of particle size.* Cancer Res. **2000**, *60*, 4440-4445.

Acta Universitatis Upsaliensis

Digital Comprehensive Summaries of Uppsala Dissertations from the Faculty of Pharmacy 196

Editor: The Dean of the Faculty of Pharmacy

A doctoral dissertation from the Faculty of Pharmacy, Uppsala University, is usually a summary of a number of papers. A few copies of the complete dissertation are kept at major Swedish research libraries, while the summary alone is distributed internationally through the series Digital Comprehensive Summaries of Uppsala Dissertations from the Faculty of Pharmacy. (Prior to January, 2005, the series was published under the title "Comprehensive Summaries of Uppsala Dissertations from the Faculty of Pharmacy".)

Distribution: publications.uu.se
urn:nbn:se:uu:diva-242893

ACTA
UNIVERSITATIS
UPSALIENSIS
UPPSALA
2015